LNG Safety Research: FEM3A Model Development

Final Report
02-25-2004 to 09-30-2006

Prepared by:

Iraj A. Salehi
Gas Technology Institute
and
Jerry Havens *and* Tom Spicer
University of Arkansas

December 22, 2006

Award No. DE-FG26-04NT42030

Submitted by:

Iraj A. Salehi
Gas Technology Institute
1700 S. Mount Prospect Rd.
Des Plaines, IL 60018

and

Jerry Havens *and* Tom Spicer
Chemical Hazards Research Center
University of Arkansas
Fayetteville, Arkansas 72701

DISCLAIMER

ABSTRACT

The initial scope of work for this project included: 1) Improving the FEM3A advanced turbulence closure module, 2) Adaptation of FEM3A for more general applications, and 3) Verification of dispersion over rough surfaces, with and without obstacle using the advanced turbulence closure module. These work elements were to be performed by Chemical Hazards Research Center (CHRC), Department of Chemical Engineering, University of Arkansas as a subcontractor to Gas Technology Institute (GTI). The tasks for GTI included establishment of the scientific support base for standardization of the FEM3A model, project management, technology transfer, and project administration. Later in the course of the project, the scope of work was modified by the National Energy Technology Laboratories (NETL) to remove the emphasis on FEM3A model and instead, develop data in support of NETL's FLUENT modeling. With this change, GTI was also instructed to cease activities relative to FEM3A model.

GTI's technical activities through this project included the initial verification of FEM3A model, provision of technical inputs to CHRC researchers regarding the structure of the final product, and participation in technical discussion sessions with CHRC and NETL technical staff. GTI also began the development of a Windows-based front end for the model but the work was stopped due to the change in scope of work. In the meantime, GTI organized a workshop on LNG safety in Houston, Texas. The workshop was very successful and 75 people from various industries participated.

All technical objectives were met satisfactorily by Dr. Jerry Havens and Dr. Tom Spicer of CHRC and results are presented in a stand-alone report included as Appendix A to this report.

TABLE OF CONTENTS

EXECUTIVE SUMMARY

1. Technical Achievements

The problems associated with instability of FEM3A in simulation of low wind speed stably stratified conditions were resolved and a new version of FEM3A, free of the aforementioned stability problems, was prepared. A second element of the work was to repeat and extend prior experiments conducted on a smooth wind tunnel floor using uniform roughness elements covering the wind tunnel floor to create turbulence properties similar to field scale wind conditions and, to develop and verify a k-epsilon turbulence closure model that allows for more realistic description of dispersion problems with obstacle and terrain effects. This objective was also met. The report by CHRC (Appendix A.) contains the data produced. A new version of FEM3A with the improved k-epsilon closure was also developed and is in the process of being provided to GTI. The modified scope of work called for provision of assistance and wind tunnel data to DOE (NETL) for FLUENT model development. This objective was met and data requested by DOE-NETL was delivered.

2. Technical and Technology Transfer Support

Technical and administrative support was provided by GTI and included the initial verification of FEM3A model, provision of technical inputs to CHRC researchers regarding the structure of the final product, and participation in technical discussion sessions with CHRC and NETL technical staff. GTI also began the development of a Windows-based front end for the model but the work was stopped due to changes in the scope of work.

Technology transfer efforts included distribution of the FEM3A and provision of technical support. In the meantime, GTI organized a workshop on LNG safety in Houston, Texas. The workshop was very successful and 75 people from various industries participated.

EXPERIMENTAL

Equipment and instruments at the wind tunnel were modified and upgraded for measurement of wind tunnel turbulence spectra as requested by NETL, as well as near-field measurements of gas concentration within the dike/tank assembly.

All experiments were carried out at the HCRC wind tunnel and included measurements with and without obstacles. Appendix A, VAPOR DISPERSION AND THERMAL HAZARD MODELING, also includes data and results from the wind tunnel experiments. The data are presented for three experimental configurations, all with the roughened wind tunnel floor surface:

- Case A – Low momentum area source CO_2 release without obstacles;
- Case B - Low momentum area source CO_2 release with dike and tank; and,
- Case C - Low momentum area source CO_2 release with dike only.

All mean velocity and concentration data are presented in tabular form in this report and are archived in the Chemical Hazards Research Center at the University of Arkansas.

Graphical summaries of the data are also presented. Cases A, B, and C all show the expected more rapid dilution in the near field followed by less rapid dilution in the far field. There are strong indications that the experimental data from the wind tunnel would be more applicable to field conditions and therefore, more useful for model validation when the floor is artificially roughened.

Parallel to activities at the HCRC, GTI began the development of a Windows-based front end for FEM3A such that it would be also used in the final software which was to be developed through this project. However, because of changes in the scope of work, these efforts were aborted. With changes in the scope of work, major technology transfer efforts were limited to organization of a workshop in which 75 people from various industries participated. The following items were covered in this workshop.

- Federal Requirements for Siting LNG Plants
- DOE's Research Programs in LNG Safety
- GTI's Research Programs in LNG Safety
- DEGADIS and LNG Fire Models: Description, Demonstration and Examples
- FEM3A : Model Description and illustrations of the model's application.

GTI will be organizing several workshops in the next two years through a separate technology transfer contract. The first of these workshops is scheduled for May, 2007.

RESULTS AND DISCUSSION

Data from experimental work was used to verify the FEM3A model for application involving dispersion over rough surfaces (for example, suburban housing) with and without the presence of obstacles such as tank and/or dike structures and industrial buildings. The end product was an advanced turbulence closure model (for describing the turbulent mixing involved in the dispersion process) that will allow for more realistic description of dispersion problems with obstacles and terrain features of greater complexity (the real world).

Researchers at CHRC utilized the FEM3A model throughout in order to consider the utility of this data for verification of CFD models, as well as to continue their own in-house improvement and maintenance of FEM3A. Based on their observations, they recommend the following considerations regarding the use of this data for verifying CFD models, and for the use of approved methods for determining LNG vapor cloud exclusion zones:

> "The wind tunnel data appears to be in best agreement in the near field, with increasing differences appearing in the (unobstructed) far field. Considering that the k-epsilon method used here would appear to be better suited to the near field calculation than the far field because its sensitivity to ad hoc provisions for density stratification, we believe that the turbulence closure approach used in the far field should be further evaluated in order to better characterize the effects upon density stratification on determinations of the turbulent kinetic energy (k) and the turbulence kinetic energy dissipation rate (epsilon).
>
> As a consequence of this finding, we recommend that FEM3A be used to determine the gas/air concentration and rate that overflows the downwind dike edge, and that the result be used as input to DEGADIS for determining the distance from the downwind edge of the dike to the ½ lfl concentration level prescribed by 49 CFR 193. We have demonstrated this method, providing further justification for this recommendation, in a recent publication in the AICHE organ Plant Safety Progress (Havens and Spicer, 2005)."

Because of the sustained high energy prices, global interest in utilization of LNG has risen to an all-time high and as such, all varieties of simulation modeling are in high demand. Data-driven validation of all models would be an imperative for reliable use of these models. We believe utilization of the wind tunnel facility should be considered in all future LNG modeling. GTI also proposes that technology transfer through workshops, in-house training, publications, and forums be considered as a critical element in utilization of these models.

GTI began the development of a Windows-based front end with appropriate GUI for FEM3A. We propose that these efforts which were aborted through the change in the scope of work be reconsidered for FEM3A and for the FLUENT model if required.

CONCLUSION

Results of the work by the HCRC researchers are presented as a stand-alone report in Appendix A. In this Appendix, wind tunnel experimental data are presented for three experimental configurations, all with the roughened wind tunnel floor surface: Case A – Low momentum area source CO_2 release without obstacles; Case B - Low momentum area source CO_2 release with dike and tank; and Case C - Low momentum area source CO_2 release with dike only. All mean velocity and concentration data are presented in tabular form and are archived in the Chemical Hazards Research Center at the University of Arkansas. Graphical summaries of the data are presented in this report.

Cases A, B, and C all show the expected more rapid dilution in the near field followed by less rapid dilution in the far field. Case B clearly demonstrates the dilution in the near field that is expected to result from the presence of obstacles (tank and dike) to the flow. Case C, importantly demonstrates that an assumption that any obstruction to the flow will result in greater dilution and corresponding shortening of the exclusion zone is by no means certain, as Case C indicates a greater downwind travel distance with the dike than

without (Case A), other factors being equal. It is believed that this result is explained by the dike restricting the gravity spreading. The importance of site roughness is clearly demonstrated. The large roughness was designed to result in a wind tunnel boundary layer that is scalable to field conditions. It is not certain that the smooth floor wind tunnel dense-gas dispersion data previously reported, although useful for limited mathematical model validation, can be scaled to field conditions. However the HCRC researchers are confident that the rough floor wind tunnel data reported herein does not suffer that weakness, and the use of data reported in Cases A, B, and C here are recommended for CFD model evaluation, either by direct simulation at wind tunnel scale, or by simulation at field (150/1) scale for comparison with the scaled wind tunnel data.

A revised version of FEM3A that does not exhibit instability when simulating low wind speed, stable atmospheric boundary layers, and which contains a k-epsilon turbulence closure model which has been verified against the wind tunnel data for Case B, is being prepared for delivery to GTI.

LNG Safety Research: FEM3A Model Development

Award No. DE-FG26-04NT42030

Final Report
02-25-2004 to 09-30-2006

Appendix A

VAPOR DISPERSION AND THERMAL HAZARD MODELING

FINAL TOPICAL REPORT

By:

Jerry Havens
Tom Spicer
Chemical Hazards Research Center
Department of Chemical Engineering
University of Arkansas
Fayetteville, Arkansas 72701 USA

VAPOR DISPERSION AND THERMAL HAZARD MODELING

FINAL TOPICAL REPORT

Prepared by

Jerry Havens
Tom Spicer

Chemical Hazards Research Center
Department of Chemical Engineering
University of Arkansas
Fayetteville, Arkansas 72701 USA

For

Gas Technology Institute
1700 S. Mount Prospect Road
Des Plaines, IL 60018-1804, USA

Contract No. 4GTI-DE-FG26-04NT42030 (Prime)
K100029184 (Subcontract)

GTI Project Manager
Iraj Salehi

October 2006

LEGAL NOTICE

This report was prepared by the University of Arkansas as an account of work sponsored by the Gas Technology Institute (GTI). Neither the University of Arkansas or GTI, members of either, or any person acting on behalf of either:

a. MAKES ANY WARRANTY OR REPRESENTATION, EXPRESS OR IMPLIED, WITH RESPECT TO THE ACCURACY, COMPLETENESS, OR USEFULNESS OF THE INFORMATION CONTAINED IN THIS REPORT, OR THAT THE USE OF ANY APPARATUS, METHOD OR PROCESS DISCLOSED IN THIS REPORT MAY NOT INFRINGE PRIVATELY OWNED RIGHTS, OR

b. ASSUMES ANY LIABILITY WITH RESPECT TO THE USE OF, OR FOR DAMAGES RESULTING FROM THE USE OF, ANY INFORMATION, APPARATUS, METHOD, OR PROCESS DISCLOSED IN THIS REPORT.

References to trade names or specific commercial products, commodities, services, or numerical models in this report do not represent or constitute an endorsement, recommendation, or opinion of suitability by GTI or the University of Arkansas of the specific commercial product, commodity, service, or numerical model.

REPORT DOCUMENTATION PAGE

1. 2/25/2004 2. 9/30/2006 3. Final Report February 2004 - September 2006

4. Vapor Dispersion and Thermal Hazard Modeling 5. Contract No. K100029184

6. Jerry Havens and Tom Spicer

7. Chemical Hazards Research Center
Department of Chemical Engineering
University of Arkansas
Fayetteville, AR 72701, USA
479-575-2055

8. Gas Technology Institute
1700 S. Mount Prospect Road
Des Plaines, IL 60018-1804, USA
847-768-0512

13. ABSTRACT

The objectives were to eliminate stability problems observed with FEM3A in simulating low-speed, stably-stratified wind flows; to extend previous experiments on a smooth wind tunnel floor using uniform roughness to create turbulence properties similar to field scale wind conditions and to develop and verify a k-epsilon turbulence closure model; and to provide assistance and wind tunnel data to DOE (NETL) for FLUENT development. A revised version of FEM3A that does not exhibit instability and which contains a k-epsilon turbulence closure model verified against the wind tunnel data for Case B presented herein is being delivered to GTI. Wind tunnel experimental data are presented here for three experimental configurations, all with the roughened wind tunnel floor surface: Case A - Low momentum area source CO_2 release without obstacles; Case B - Low momentum area source CO_2 release with dike and tank; and Case C - Low momentum area source CO_2 release with dike only. Mean velocity and gas concentration data are presented in tabular form. The importance of site roughness is clearly demonstrated. The wind tunnel data appears to be in best agreement with CFD models (FEM3A) in the near field, with increasing differences appearing in the (unobstructed) far field. Considering that the k-epsilon method used here appears better suited to the near field calculation than the far field, presumably because of its sensitivity to ad hoc provisions for density stratification, we are recommending that for LNG vapor cloud exclusion zone determination for spills into impoundments or diked areas, FEM3A be used to determine the gas/air concentration and rate that overflows the downwind dike edge, and that the result be used as input to DEGADIS to determine the downwind distance to the ½ lfl concentration level.

RESEARCH SUMMARY

Title	Vapor Dispersion and Thermal Hazard Modeling
Contractor	University of Arkansas
Contract Number	K100029184
Principal Investigators	Jerry Havens and Tom Spicer
Report Type and Period	Final April 2004 - September 2006
Objectives	The first objective was was to eliminate stability problems that had been observed in FEM3A simulations of low-wind-speed, stably-stratified conditions. This objective was met and a new version of FEM3A, free of the aforementioned stability problems, is being provided to GTI. The second objective was to repeat and extend prior experiments conducted on a smooth wind tunnel floor using uniform roughness elements covering the wind tunnel floor to create turbulence properties similar to field scale wind conditions and to develop and verify a k-epsilon turbulence closure model that allows for more realistic description of dispersion problems with obstacle and terrain effects. This objective was met; this report contains the data produced, and a new version of FEM3A with the improved k-epsilon closure is being provided to GTI. The third objective was to provide assistance and wind tunnel data to DOE (NETL) for FLUENT development. This objective was met and data requested by DOE-NETL was delivered
Results	A revised version of FEM3A that does not exhibit instability when simulating low wind speed, stable atmospheric boundary layers, and which contains a k-epsilon turbulence closure model which has been verified against the wind tunnel data for Case B presented herein is being delivered to GTI. Wind tunnel experimental data are presented here for three experimental configurations, all with the roughened wind tunnel floor surface: Case A - Low momentum area source CO_2 release without obstacles; Case B - Low momentum area source CO_2 release with dike and tank; and Case C - Low momentum area source CO_2 release with dike only. All mean velocity and concentration data are presented in tabular form in this report and are archived in the Chemical Hazards Research Center at the University of Arkansas. Graphical summaries of the data are presented in this report. Cases A, B, and C all show the expected more rapid dilution in the near field followed by less rapid dilution in the far field. Case B clearly

demonstrates the dilution in the near field that is expected to result from the presence of obstacles (tank and dike) to the flow. Case C, importantly, demonstrates that an assumption that any obstruction to the flow will result in greater dilution and corresponding shortening of the exclusion zone is by no means certain, as Case C indicates a greater downwind travel distance with the dike than without (Case A), other factors being equal. We believe that this result is explained by the dike restricting the gravity spreading. The importance of site roughness is clearly demonstrated. The large roughness used here was designed to result in a wind tunnel boundary layer that is scalable to field conditions. We are not confident that the smooth floor wind tunnel dense-gas dispersion data previously reported, although useful for limited mathematical model validation, can be scaled to field conditions. However we are confident that the rough floor wind tunnel data reported herein does not suffer that weakness, and the use of data reported in Cases A, B, and C here are recommended for CFD model evaluation, either by direct simulation at wind tunnel scale, or by simulation at field (150/1) scale for comparison with the scaled wind tunnel data.

Project Implications

We have utilized the FEM3A model throughout in order to consider the utility of this data for verification of CFD models, as well as to continue our own in-house improvement and maintenance of FEM3A. The wind tunnel data appears to be in best agreement in the near field, with increasing differences appearing in the (unobstructed) far field. Considering that the k-epsilon method used here would appear to be better suited to the near field calculation than the far field because its sensitivity to ad hoc provisions for density stratification, we believe that the turbulence closure approach used in the far field should be further evaluated in order to better characterize the effects upon density stratification on determinations of the turbulent kinetic energy (k) and the turbulence kinetic energy dissipation rate (epsilon). As a consequence of this finding, we recommend that when used for LNG vapor cloud exclusion zone determination for spills into impoundments or diked areas, FEM3A be used to determine the gas/air concentration and rate that overflows the downwind dike edge, and that the result be used as input to DEGADIS to determine the distance from the downwind edge of the dike to the ½ lfl concentration level as prescribed by 49 CFR 193.

TABLE OF CONTENTS

TABLE OF CONTENTS (Appendix II continued)

LIST OF FIGURES

LIST OF FIGURES (continued)

1.0 BACKGROUND AND OBJECTIVES

Federal requirements for vapor cloud dispersion exclusion zones around LNG storage and transfer facilities direct the use of dispersion models specified in 49 CFR 193. The dispersion model required in 49 CFR 193 (promulgated in 1980) was a line-source Gaussian (passive) dispersion model ("the MTB model"; Arthur D. Little, Inc., 1974) which did not account for LNG vapor negative buoyancy (LNG vapor, because of its low temperature, can be denser than air). Neither did the MTB model provide for consideration of (earth) surface-to-cloud heat transfer, holdup in vapor detention systems (such as by impoundments, dikes, and vapor fences), wake turbulence, or directional diversion of vapor clouds by topography. It was recognized that modeling tools that would take into account all of these factors were required in order to address important issues facing the industry in determining safety exclusion zones to protect the public from vapor clouds that might be formed from LNG releases, particularly at land-based facilities where such site specific factors are expected to be important.

The Gas Research Institute (GRI) sponsored research to develop and verify alternative dispersion modeling approaches which might be substituted for the initially prescribed passive dispersion model (Havens et al., 1987; Havens and Spicer, 1990; Havens et al., 1994, Spicer and Havens, 1996). GRI defined two major objectives for the development of alternative vapor dispersion methods for regulatory use (specifically in 49 CFR 193):

- The first objective was to define "short-cut" methods for determining exclusion zones for site selection screening, tentative compliance evaluations, and applications where minimization of exclusion area is not as crucial (such as for small plants located in rural areas). This objective was accomplished when 49 CFR 193 was amended in 1992 to require the use of the DEGADIS (DEnse GAs DISpersion) model in place of the originally prescribed model (Havens and Spicer, 1990). The DEGADIS model accounts for LNG vapor negative buoyancy as well as for consideration of the effect of (earth) surface-to-cloud heat transfer on atmospheric turbulent mixing. However, being a "flat-earth" model, it does not provide for vapor cloud liftoff or effects on vapor cloud dispersion of any kind of obstacles (man-made or natural) to wind or vapor cloud flow.

- The second objective was to define procedures for regulatory applications where topographical effects, wake turbulence, vapor holdup in detention systems, and energy addition (heat transfer and moisture condensation) to the cloud, including cloud liftoff due to positive buoyancy, considered separately or in combination, might be expected to importantly influence exclusion zone requirements. This objective was accomplished when 49 CFR 193 was amended in 2001 to allow the use of the FEM3A model as an alternative to DEGADIS <u>if the applicant desired to consider the effect upon dispersion of man-made or natural obstacles (to the flow) such as dikes or tanks or terrain features</u> (Spicer and Havens, 1996).

Reports by Havens, Spicer and Walker (1996), submitted to the Department of

Transportation (DOT) as supporting documentation for the amendment of CFR 193 to allow use of FEM3A, present the results (to 1996) of the extensive research program conducted to develop accurate, repeatable laboratory (wind tunnel) data sets which begin to effectively address realistic LNG vapor dispersion scenario issues and which could be used to evaluate the predictability of LNG vapor dispersion mitigation with FEM3A or other computational fluid dynamic (CFD models). The research program was cosponsored (with GRI) by the following organizations:

- British Gas
- ENAGAS (Spain)
- Gaz de France
- Mitsubishi Heavy Industries, Ltd. (Japan)
- Osaka Gas Company (Japan)
- TNO (The Netherlands)

Data sets were provided to evaluate mathematical models applicable to the prediction of the following laboratory (wind tunnel) scale dense gas dispersion scenarios:

- Phase 1 - isothermal dense gas released continuously (steady state) with near-zero momentum from a floor-level area source.

- Phase 2 - isothermal dense gas released continuously (steady state) with near-zero momentum from a floor-level area source in the annular space within a dike surrounding a storage tank.

- Phase 3 - cryogenic dense gas released continuously (steady state) with near-zero momentum from a floor-level area source.

The report of this work by Havens, Spicer, and Walker (1996), Evaluation of Mitigation Methods for Accidental LNG Releases, consists of five volumes:

1. Wind Tunnel Experiments and Mathematical Model Simulations to Study Dispersion of a Vapor Cloud Formed Following LNG Spillage into a Diked Area Surrounding a Storage Tank.

2. Wind Tunnel Experiments and Mathematical Model Simulations to Study Heat Transfer from a Flat Surface to a Cold Nitrogen Cloud in a Simulated Atmospheric Boundary Layer.

3. Wind Tunnel Experiments for Mitsubishi Heavy Industries, Ltd.

4. Wind Tunnel Experiments for Osaka Gas Company.

5. Using FEM3A for LNG Accident Consequence Analysis. (Vol. 5 was the

original users's manual supplied to DOT for the FEM3A model specified in 49 CFR 193.)

Following agreements by GRI and the Lawrence Livermore National Laboratory (LLNL), the FEM3A model is licensed by the Gas Technology Institute (GTI), formed by merger of the Institute of Gas Technology (IGT) and the Gas Research Institute (GRI). Then, following approval by DOT of the FEM3A model for determining vapor cloud exclusion zones as required by 49 CFR 193, GTI and the University of Arkansas conducted additional research to provide for maintenance and improvement of the FEM3A model (Havens and Spicer, 2003).

In 2004, The University of Arkansas began the contract for which this final report is submitted. The primary contract was between the Department of Energy National Energy Technology Laboratory (NETL) and GTI. The University of Arkansas was subcontractor to GTI. The primary objective of the University's contract was initially to develop the FEM3A dispersion model for application to general scenarios involving dispersion problems with obstacle and terrain features of realistic complexity, and for very low wind speed, stable weather conditions as may be required for LNG vapor dispersion application specified in 49 CFR 193. The subcontract specified three principal tasks:

Task A – Simulation of Low-Wind-Speed Stable Atmospheric Conditions

It was necessary to validate the FEM3A model with data from neutral stability wind tunnel boundary layer experiments, since suitable experimental facilities for simulating a stable boundary layer (at the required scale) in a wind tunnel have not been demonstrated. Furthermore, the FEM3A code had not been applied previously for such conditions, and calculations at the University of Arkansas had shown that FEM3A simulations of stably stratified conditions were subject to numerical stability problems. Task A was to eliminate the stability problems that had been observed in simulations of low-wind-speed, stably-stratified conditions. This was a high priority requirement since the application of the code for compliance with the regulation can require simulations to be made for such conditions, which are sometimes worst case.

Task A was completed, and a new version of FEM3A, free of the aforementioned stability problems, is being provided to GTI.

Task B – Verification for Dispersion over Rough Surfaces, With and Without Obstacles

All previous experiments in the CHRC wind tunnel to validate the FEM3A model for prediction of the effect of the presence of tank and dike structures had utilized a smooth wind tunnel floor. However, further evaluation of that early work indicated that the presence of the smooth floor combined with the low wind speeds required to simulate the dense gas effects involved in LNG vapor dispersion can result in the tendency for the boundary layer near the floor to laminarize. Although such effects could be considered in the mathematical models so as to account for laminarization at wind-tunnel scale, thus

providing for verification of the model using wind tunnel experiment data, such conditions make suspect the scaling of the wind tunnel flows to field scale because field conditions are normally fully turbulent (laminarization does not normally occur at field scale). There were strong indications that the experimental data from the wind tunnel would be more applicable to field conditions, and therefore more useful for model validation, if the floor were artificially roughened. Consequently, the primary purpose of this task was to repeat and extend former experiments using uniform roughness elements covering the wind tunnel floor to create turbulence properties similar to field scale wind conditions. There were to be two important by-products planned from this task:

- A k-epsilon turbulence closure model (for describing the turbulent mixing involved in the dispersion process) that allows for more realistic description of dispersion problems with obstacle and terrain features (the real world).

- A valuable addition of rough surface wind tunnel boundary layer data to the archives that are applicable to the verification of CFD models which may be proposed as alternatives to FEM3A for such use.

Task B was completed. This report contains the data produced, and a new version of FEM3A with the improved k-epsilon closure is being provided to GTI.

Task C – Adapting the FEM3A Model for More General Application

As more complex applications of the FEM3A model are proposed, it was anticipated that there will be additional questions related to model evaluation and verification that can best be addressed by experimentation in the CHRC wind tunnel. Examples of complex scenarios that were anticipated were evaluation of vapor fences for containment of flammable gases and aerosols, scenarios containing multiple obstacles, and major terrain features. However, near the mid-point of the contract period, DOE redirected this effort in order to provide CHRC's assistance to DOE-NETL in their consideration of the FLUENT CFD model as an alternative (to FEM3A) model for use under 49 CFR 193. Consequently, this task was obviated, and Task D was added.

Task D - Provide assistance and wind tunnel data to DOE for FLUENT development

Task D was completed and data requested by DOE-NETL was delivered.

2.0 DESCRIPTION OF THE EXPERIMENTAL FACILITY

The ultra-low-speed (ULS) wind tunnel at the Chemical Hazards Research Center (CHRC) was designed and constructed specifically for the study of atmospheric dispersion of denser-than-air gases at wind tunnel speeds below 2 m/s (Havens, Spicer, and Walker, 1996). A description of the tunnel is presented first, followed by a description of the principal instrumentation used in the work described herein.

CHRC ULS Wind Tunnel

The ULS tunnel is an ultra-low-speed boundary layer wind tunnel capable of producing airflows that simulate the constant stress layer of the atmospheric boundary layer (ABL). Figure 1 depicts the floor plan of the CHRC Wind Tunnel. As shown in the diagram, the wind tunnel is centered laterally in a larger room in order to ensure a symmetrical return space for the recirculating air on both sides, under, and over the tunnel. An isolated control/observation room is situated adjacent to the wind tunnel containing data acquisition systems and control instrumentation. During the course of an experiment, the tunnel room is isolated so as to prevent extraneous effects that would disrupt the tunnel flow and the variables being measured.

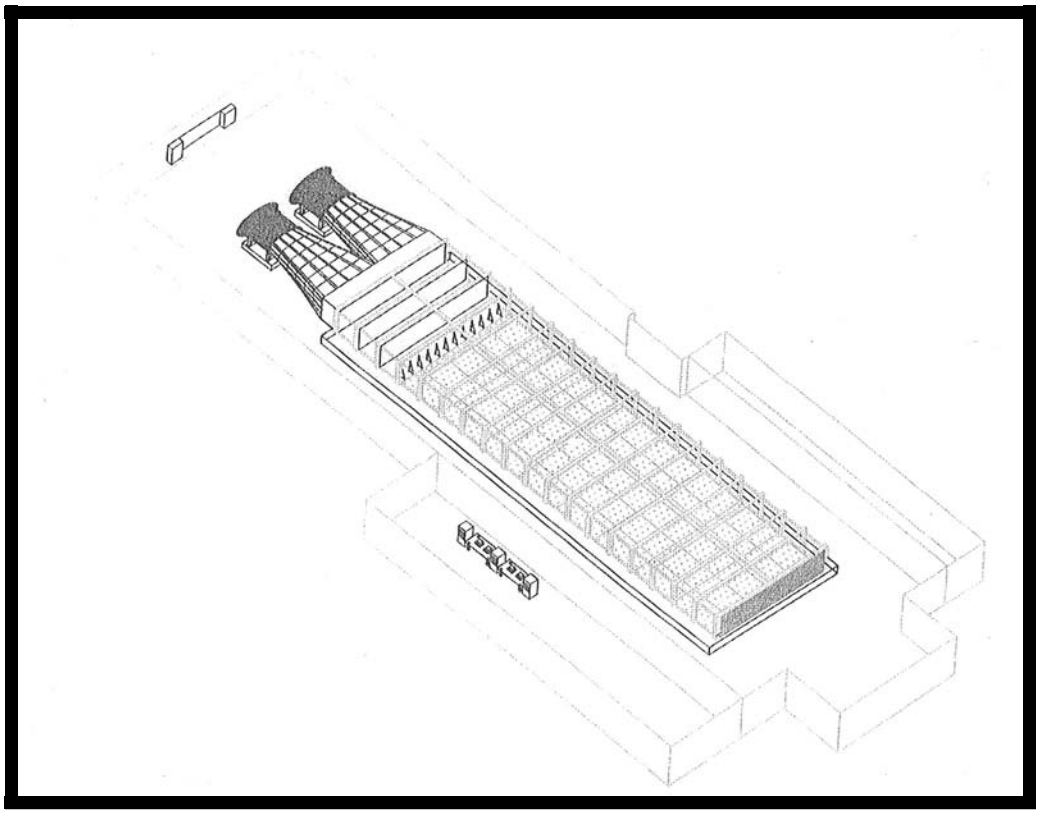

Figure 1. Floor plan of CHRC ULS wind tunnel

Two 75-horsepower, 72-inch diameter adjustable pitch vane-axial fans, manufactured by Buffalo Forge Company, provide the "push-through" (recirculating) airflow. The fans, working as master-and-slave and outfitted with Fenner M-Trim speed controllers, provide for regulation of the rotational speed in revolutions-per-minute (rpm) by a computer-based control system in the control room. The speed of each fan is monitored by an optical sensor and displayed by a digital tachometer in the control room. See Appendix I, Figure I-1 for illustration.

The airflow produced by the fans passes through a circular-to-rectangular transition from the fans to the working area (7 ft height x 20 ft width x 80 ft length) of the wind tunnel (See Appendix I, Figure I-2 for illustration). This working area is divided into two regions; the boundary-layer-generation region, and the measurement region.

The boundary-layer-generation region follows immediately after the circular-to-rectangular transition. The air flows through a honeycomb consisting of ½ -inch size cells, "straightening" the flow and removing large scale turbulence. Four seamless nylon screens placed after the honeycomb further reduce turbulence in the airflow, generating a uniform airflow across the cross-sectional area of the wind tunnel. A turbulent boundary layer is induced by fourteen Irwin spire-shaped turbulence generators (13.2 cm base, and 92.7 cm height; Figure 2) positioned 30 cm downwind from the last screen, with 46.3 cm between adjacent spires. The measurement region begins six spire heights (approximately 18 ft) downwind from the spires. The floor of the tunnel was tiled with smooth rubber matting. Several experiments involving velocity and gas concentration measurements were performed over the smooth floor

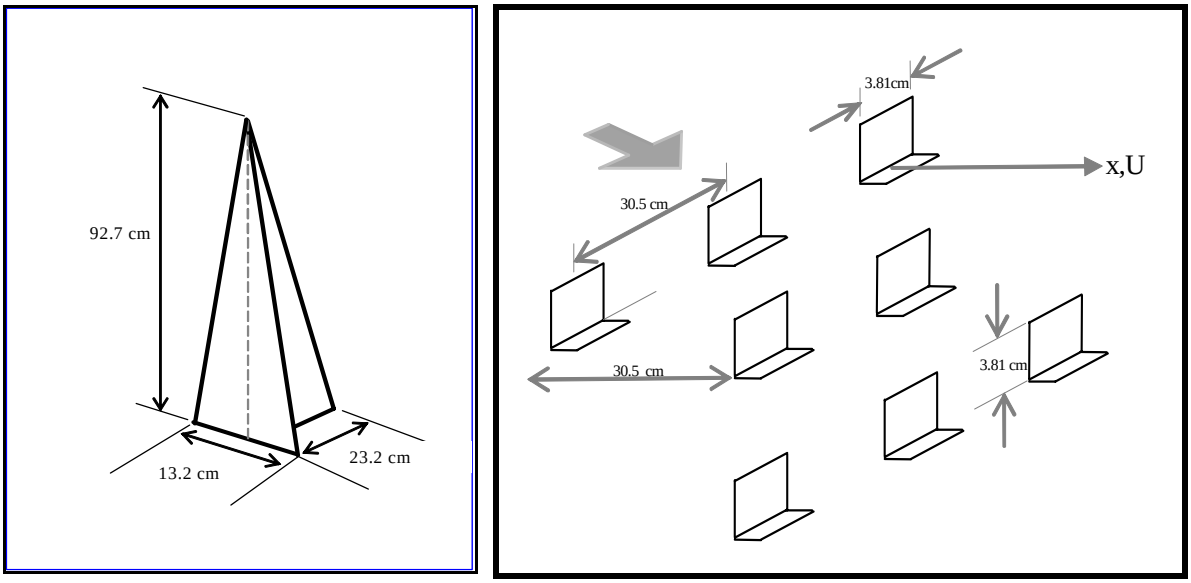

Figure 2. Details of turbulence generators and surface roughness

(used in early experiments) to verify repeatability. Subsequently, cut aluminum angles functioning as surface roughness elements were installed on the floor to "roughen" the floor in

the boundary-layer-generation and measurement region (See Figure 2 for details of the roughness; Appendix I, Figure I-3 for illustration).

At the end of the working section of the tunnel another seamless screen and a back-pressure device consisting of vertical Plexiglass strips, 3 inches in width and 1/4 inch in thickness spaced 3-3/16 inches apart, were installed. See Appendix I, Figure I-4 for illustration.

Modeling System

Roughness elements (Figure 2) were installed on the floor surface of the wind tunnel. All of the surface roughness elements were made of cut aluminum angle with a square base of 3.81 cm in length on all sides with another square of the same dimensions extending perpendicularly from one edge of the base. The elements were arranged in a staggered array at a distance of 30.5 cm between subsequent elements in the downwind and lateral directions.

A 150:1 scale model of the tank and dike configuration (See Figure 3, and Appendix I, Figures I-5 and I-6 for details) was installed in the tunnel. The tank was 31 cm in diameter, cylindrical in shape, and had a spherical-section "dome" top. The height of the tank measured to the top of the dome was 28.3 cm. The areas enclosed by the dikes were square in shape, with the tank located in the center. The inner side-length dike dimension was 0.636 m, and the dike height was 0.037 m. The tank was placed on a platform topped with a mesh screen that was flush with the tunnel floor surface.

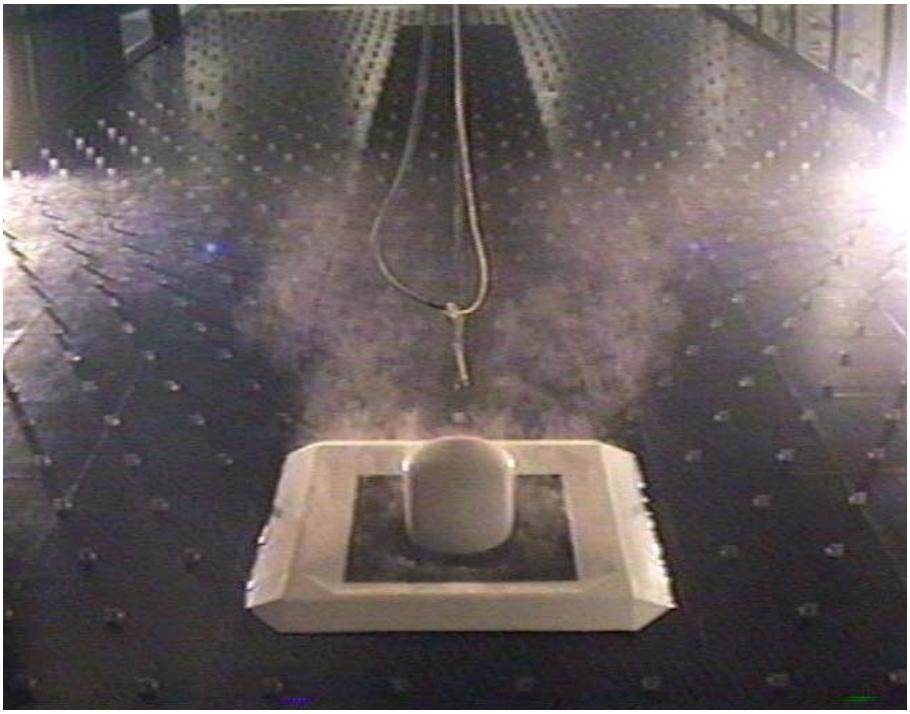

Figure 3. Tank and dike model placement in wind tunnel, with roughness - flow visualization

The platform on which the tank rested was placed on the floor of a 46.75 inch (inside dimension) square Plexiglas walled box fitted into the wind tunnel floor with the open top of the box positioned flush with the wind tunnel floor surface (Figure 4). The depth of the box was 15 inches. Gas introduced into the bottom of the box flowed vertically through six equally spaced horizontal screens before flowing through the screen into the tunnel at the tunnel floor surface.

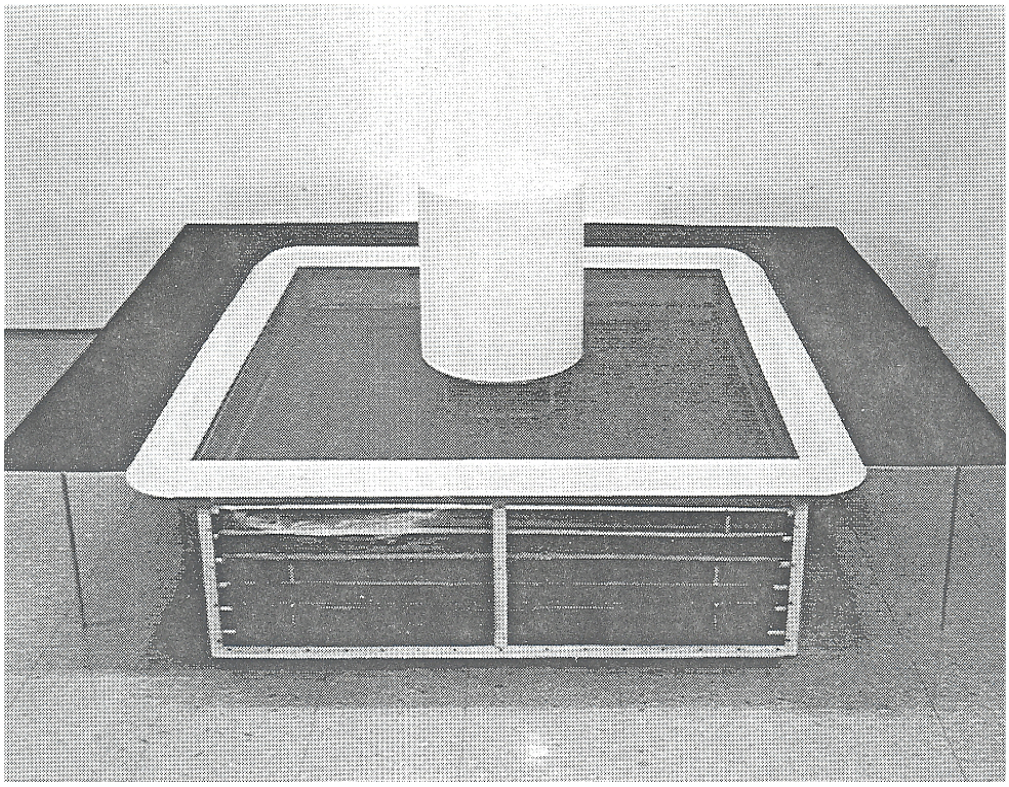

Figure 4. (Cutaway) Illustration of Gas Box Placement in Wind Tunnel Floor.

Gas Mass Flow Control System

The gases used in the experiments (carbon dioxide and propane tracer) were supplied from pressure cylinders connected via 1/2-inch plastic tubing to MKS flow controllers. Four individual mass flow controllers (MFC) were controlled by an MKS Multi-Gas Controller. The mass flow controllers used in the experiment were one Matheson MFC calibrated for nitrogen at a full range of 10 standard liters per minute, Two MKS MFC's (Model 1259C) calibrated for nitrogen at a full range of 5 standard liters per minute, and one MKS MFC (Model 1559C) calibrated for nitrogen at a full range of 50 standard liters per minute. The Matheson MFC was used to control the mass flow of air used in the experiment, the MKS 1259C MFC's were used to control mass flows of a carbon dioxide slipstream and propane, and the 1559C was used to control the main carbon dioxide flow. The four mass flow controllers were connected to the Model 647A MKS Multi-Gas Controller.

Velocity Measurement

Measurements of wind tunnel velocity and turbulence statistics utilized constant temperature thermal anemometry (CTA) hot-wires, specifically miniature cylindrical two-sensor "X"-film probes (Model Number 1248A-10 by TSI, Inc. (Figure 5a). Figure 5b shows a side view photograph of the constant-temperature hot-wire anemometer probe mounted the in the wind tunnel. The X-probe simultaneously measures two components of the velocity vector. The XWA probe support was hooked up to a micro-electric motor that was capable of orienting the probe in two perpendicular positions to allow alternative measurement of velocities in the x-y and x-z directions. The changes in orientation were remotely controlled from the control room.

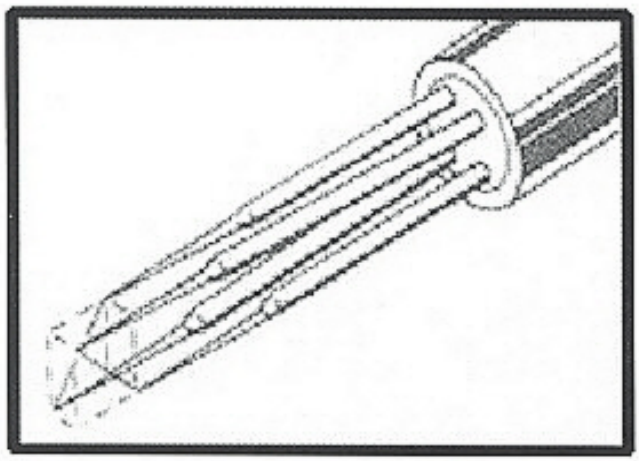

Figure 5a. Schematic of XWA film probe

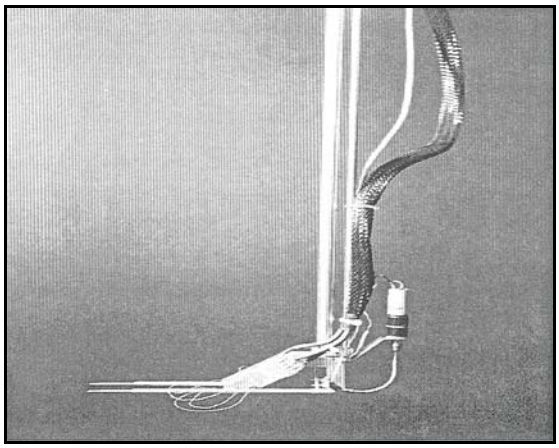

Figure 5b. XWA probe

Gas Concentration Measurement

A high frequency response HFR-400 fast flame ionization detector (FID) by Cambustion Limited (UK) was used to make the gas concentration measurements. This application was based on the physical phenomenon that significant quantities of ions are produced when a hydrocarbon is burned, thus making it possible to detect the hydrocarbon tracer in the sample gas. Propane (1.475%) was used as the hydrocarbon tracer gas in the experiments described here.

Figure 6 shows a side view photograph of the FID gas probe mounted on a traverse arm in the wind tunnel. It consisted of a sampling head, a gas-handling subsystem, and an electronics system. The sampling head contained the burner assembly to which the hydrogen fuel gas, air and sample gas were supplied in order to produce the

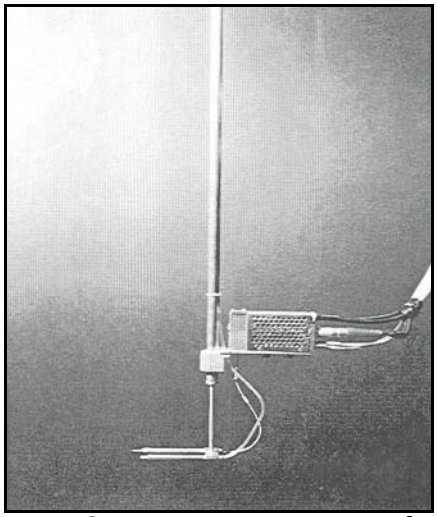

Figure 6. FID concentration probe

flame at the glow plug in the FID chamber. The flows of the gases were carefully regulated via capillary tubes and pressure regulators. The negative ions generated in the flame were collected at the insulated collector electrode, and an electrical signal which was nearly proportional to the number of carbon atoms present in the flow was generated. The signal was then converted to a voltage output and processed for gas concentration by a personal computer.

Data Acquisition System

Figure 7 shows the layout of the data acquisition system. The output voltages from the XWA and the FID were routed to the IFA 300 Control Unit (TSI Inc.) The IFA 300 was equipped with built-in signal conditioning circuitry and a thermocouple circuit for measuring fluid temperature. The unit also contained a microprocessor that stored information on the functions and settings of the anemometer and signal conditioner. A model 6260 Direct Memory Access (DMA) interface card was used to transmit data as a 12-bit mantissa and a 4-bit exponent. The data were transmitted to the computer via an RS-232 interface. The computer, equipped with an analog to digital converter, was a 486 33 MHz PC with a 1 gigabyte hard drive.

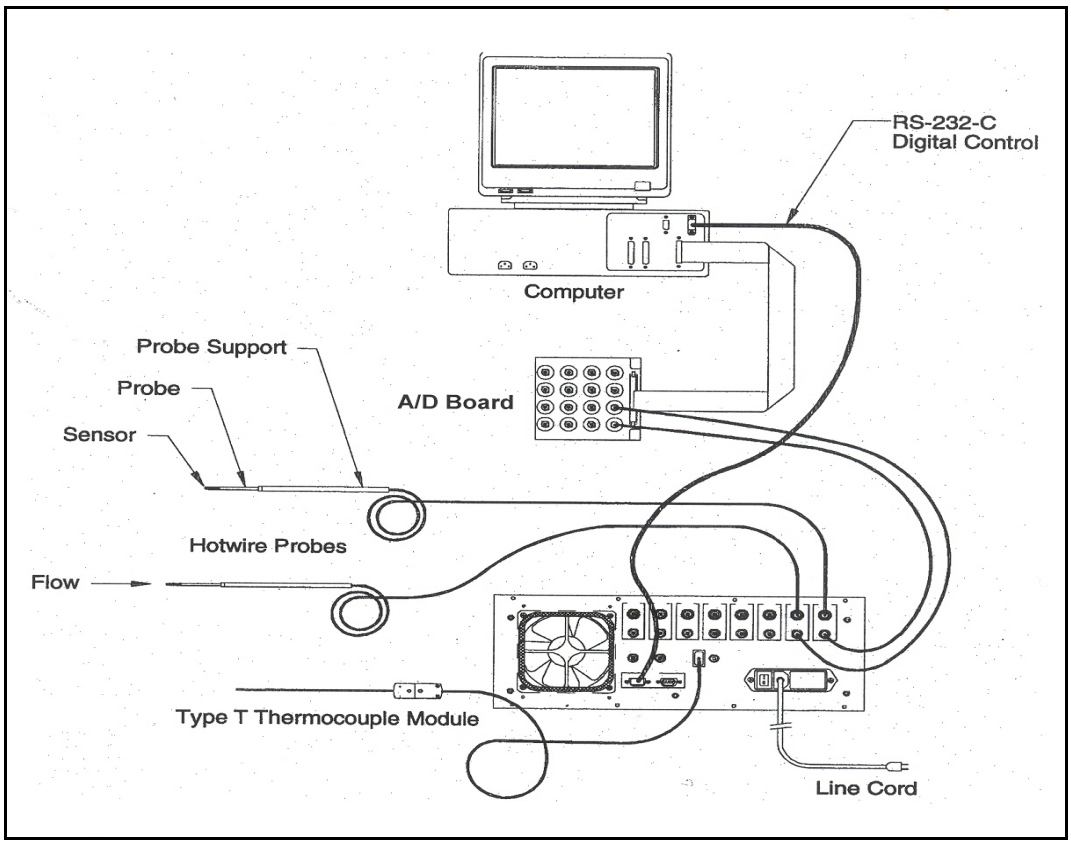

Figure 7. Layout of data acquisition system

3.0 DESCRIPTION OF EXPERIMENTS

This report contains wind tunnel data including approach (mean) flow wind velocity and gas concentrations for three wind tunnel experimental configurations (Cases A - C); all at 150 to 1 (field to wind tunnel) scale with roughened wind tunnel floor:

Case A. Low momentum area source CO_2 release without obstacles
Case B. Low momentum area source CO_2 release with dike and tank
Case C. Low momentum area source CO_2 release with dike only

The gas released for all experiments reported here was 33.4 standard liters per minute (slpm) CO_2 mixed with 0.5 slpm C_3H_8 tracer (to enable measurement of gas concentration with the flame ionization detector). The gas release source area was 0.3341 m^2 for all three cases. The tank was 31 cm in diameter with a spherical-section dome 28.3 cm high at the center. A detailed description of the tank and the dike design is provided in Appendix I. Details of the surface roughness were presented in Section 2.0 of this report.

Flow Visualization Tests

Visualization Tests for Cases A and B were conducted prior to the experimental measurement phase to demonstrate the symmetry of the flow in the tunnel. Visualization of the clouds was accomplished by adding Rosco fog (theater) fluid to the carbon dioxide at the entrance to the source box under the tunnel. Fog fluid addition was at the same rate, as nearly as could be approximated, for all tests. A video camera was mounted near the center of the tunnel ceiling so as to give an oblique view of the gas flowing in the downwind direction. Camera position and angle of view were the same for both tests. Figures 8 - 9 shows video frames representing Cases A and B. Visualization tests were not considered necessary when Case C was studied.

Velocity Measurements

The wind tunnel fans were run at 90 RPM for approximately one hour prior to commencement of measurements. Other preparatory steps included ascertaining that the air-conditioners in the wind tunnel area were turned off, ensuring that sufficient gas was available for the calibration and measurement phases of the experiment, positioning the XWA probe at calibration height, centering the XWA probe in the outlet of the calibration tube, and setting up daily records in the laboratory notebooks. The values for temperature, pressure, and relative humidity in the wind tunnel were recorded. All entries to and exits from the wind tunnel area were closed prior to the commencement of each experiment.

The calibration tube used to calibrate (for velocity) the XWA sensor was a 0.5-inch diameter, 30 inch long, Plexiglass tube. Breathing-grade bottled air was used. The flow rates were regulated by the Matheson mass flow controller in the Mass Flow Control System described in Section 2. The specific flow rates used in the calibration were designed to provide laminar

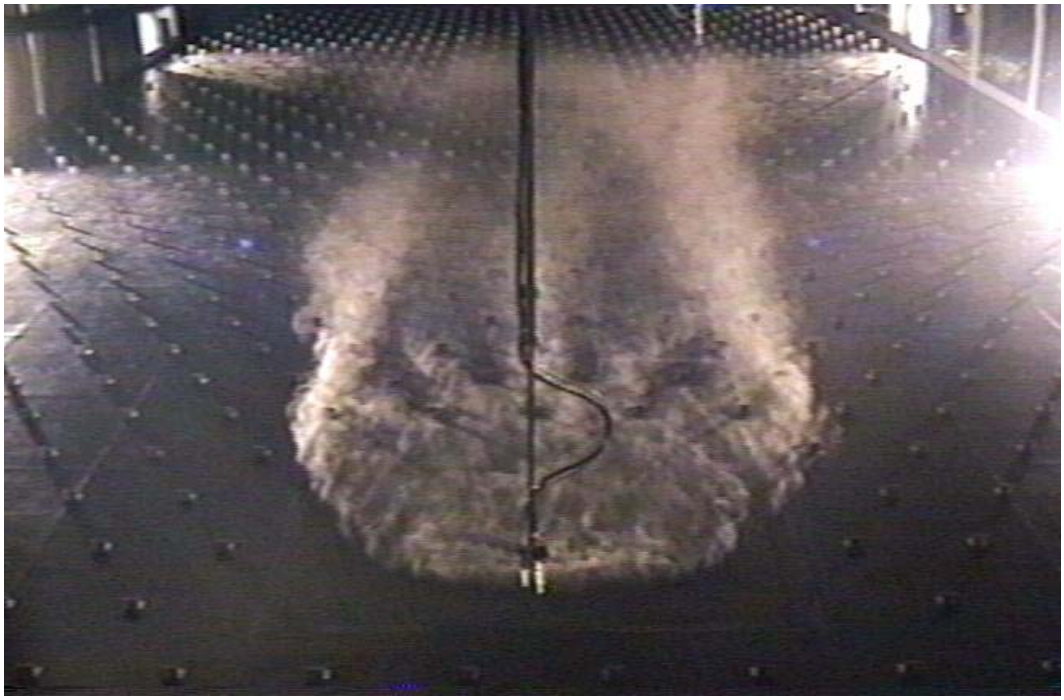

Figure 8. Flow visualization for Case A

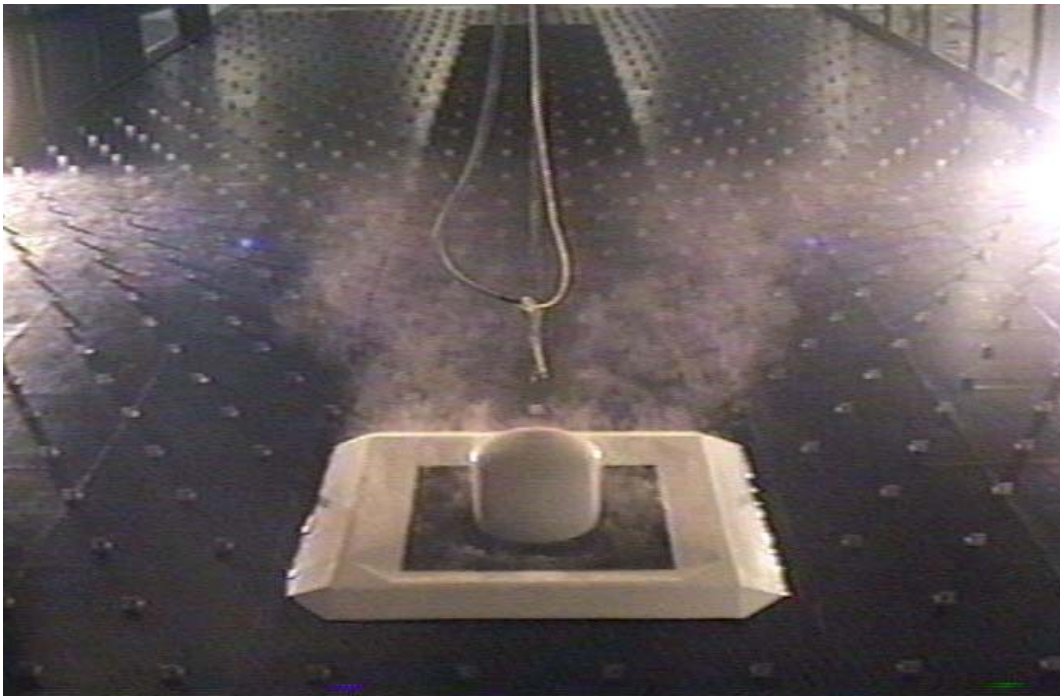

Figure 9. Flow visualization for Case B

flows through the tube that spanned the range of the wind velocities studied in the experiments. The centerline velocities in the calibration tube detected by the XWA sensor were consequently twice the value of the average velocities.

A typical calibration curve for the XWA which is illustrative of both of the (cross) wires is shown in Figure 10. The fans were turned off during the calibration to eliminate external effects during the calibration of the XWA. The XWA was calibrated by decoupling it as if it were two single probes, and data were acquired using the "acquisition" function of IFA 300 ThermoPro software. Each data point in the calibration stage was taken at 1000 Hertz for 60 seconds. Ten voltage (calibration points) were obtained corresponding to flow rates between 0.5 slpm and 2.3 slpm with 0.2 slpm increments.

Eleven voltage calibration points were measured at the highest flow rate (2.3 slpm), corresponding to 6-degree increment angles between 30 degrees right and 30 degrees left, for the yaw calibration of the XWA. The angular dependence required for the yaw calibration was achieved by pivoting the calibration tube about the centerline location of the XWA.

Following computer processing of the raw data files, the voltages with their corresponding flow rates for the velocity calibration were then entered into the software to generate two separate calibration curves, one for each of the "X" wires. Mean-square-errors for both curves were also shown as an indication of the deviation of the calibration curve from a fourth-order polynomial. The voltages from the yaw calibration were also entered into the software to calculate the yaw coefficients.

The XWA probe was positioned at an elevation of 0.5 (+/- 0.1) cm above the floor for all measurements in this study. In some cases, additional data points were taken (on the centerline of the wind tunnel) at elevations of 0.95, 1.5, 2.3, 3.3, 4.6, 6.3, 8.5, 11.5, 15, and 20 cm. Two data points were acquired at each measurement position (by rotating the XWA probe 90 degrees), so that the U-mean (downwind) velocities were repeated. The mean turbulence statistics, including mean velocities reported here, were determined from data sampled at 1 kHz for 2 minutes.

Gas Concentration Measurements

The fans were run at 90 RPM for approximately one hour prior to commencement of measurements. Preparatory activities included lighting the FID and allowing a one hour period for it to stabilize, setting the FID (chamber) temperature in the range 285-300 ^{o}C, and setting the pressure drop across the sample tube at approximately 290 mm Hg. As before, the wind tunnel area was isolated to prevent external disturbances of the flow in the tunnel, and temperature, pressure, and relative humidity were recorded.

A typical gas concentration calibration curve is shown in Figure 11. The fans were set to zero RPM (the motors continued to run) during the gas calibration. A calibration line "diffuser" was constructed of a 6 inch long, 1 inch diameter Plexiglass tube fitted with a cotton or porous foam filter which damped pressure fluctuations in the calibration gas supply. Calibration entailed

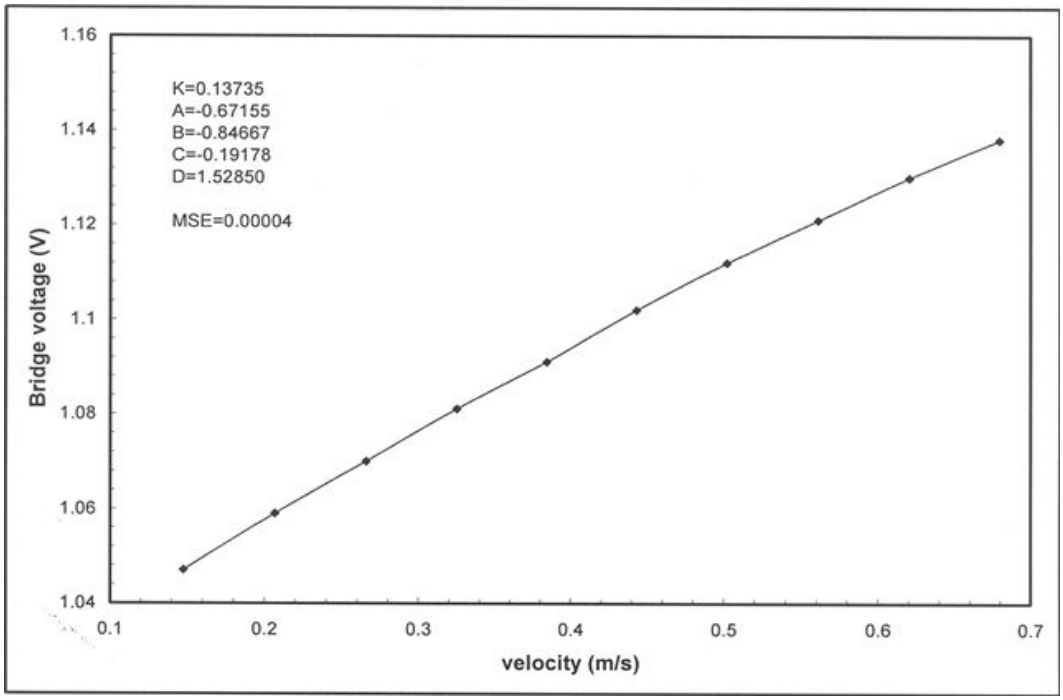

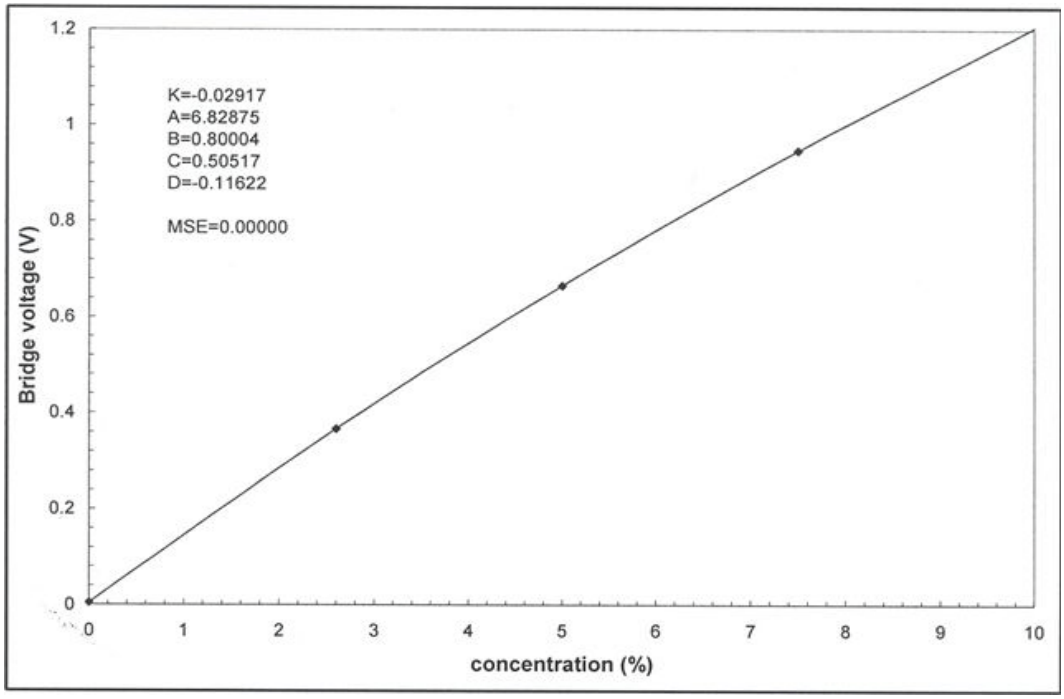

Figure 10. Typical XWA velocity probe calibration (top)
Figure 11. Typical FID concentration probe calibration (bottom)

generating a five-point calibration curve. Data for each calibration point were sampled at 1kHz for 60 seconds for air-CO_2 mixtures (using propane tracer) corresponding to carbon dioxide concentrations of 0%, 14%, 20%, 25%, and 30%. The 0% point was taken in the room air at the beginning of each experiment, so as to subsequently measure concentrations relative to the initial room gas air mixture (of air, carbon dioxide, and minor hydrocarbon contaminants). Subsequent data points were measured by inserting the sampling tube into the calibration diffuser (perpendicular to the flow in the diffuser).

Following calibration, the fans were reset to 90 RPM and gas flow to the source box under the wind tunnel floor was started. The flow for all experiments was set at 33.4 slpm carbon dioxide traced with 0.5 slpm (~1.5%) propane. Gas flow downwind of the source box reached steady state in approximately 30 minutes (after filling the source box), and the gas concentration measurements were begun.

Lateral profiles of gas concentration were made at preassigned downwind locations. All of the lateral profile measurements were made at 0.5 cm elevation, the closest practicable position above the floor surface. The lateral profiles spanned the entire gas cloud with a 10 cm lateral interval between measurement locations. In selected experiments, vertical gas concentration profiles were measured on the wind tunnel centerline; these profiles were taken with data points at 0.5 cm vertical intervals so as to span (vertically) the gas cloud down to concentrations of approximately 1%.

4.0 EXPERIMENTAL RESULTS

Data are presented here for three experimental configurations, all with the roughened wind tunnel floor surface:

Case A. Low momentum area source CO_2 release without obstacles
Case B. Low momentum area source CO_2 release with dike and tank
Case C. Low momentum area source CO_2 release with dike only

All mean velocity and concentration data are presented in tabular form in Appendix II, and are archived in the Chemical Hazards Research Center at the University of Arkansas. Graphical summaries of the data are presented here.

Velocity Data

Measurements were made of the vertical profile of mean velocity and turbulence statistics on the centerline of the wind tunnel immediately upwind of the gas source box. These data were used to determine the mean velocity at the (model) elevation corresponding to 10 meters elevation at field scale (1000 cm/150 = 6.67 cm) as well as to determine the friction velocity and the surface roughness.

Figure 12 shows measurements of the upwind, approach flow, velocity profile over the roughened wind tunnel floor. All of the experiments reported here were for this approach flow velocity profile.

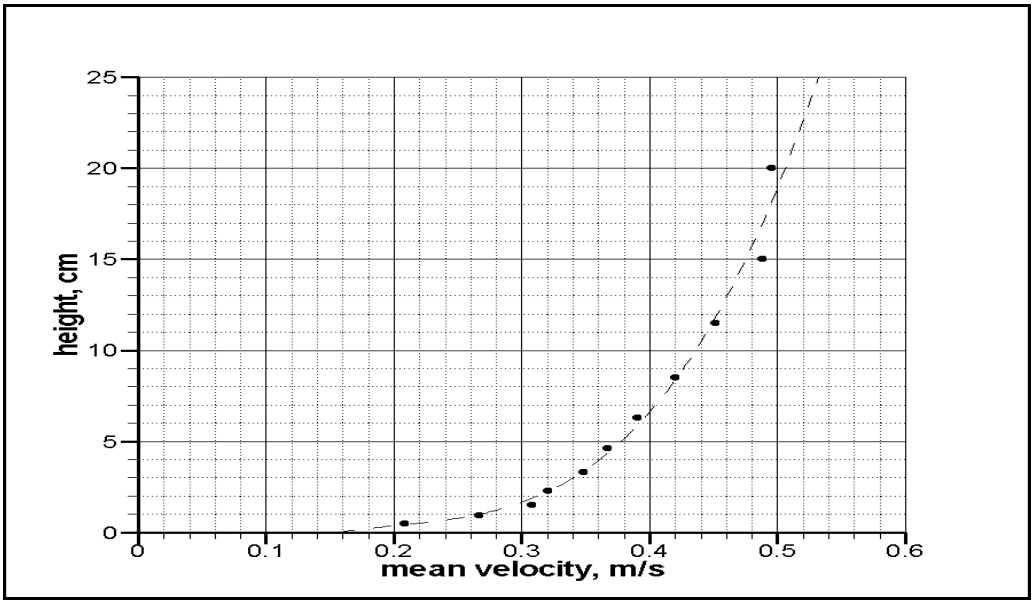

Figure 12. Rough floor, approach flow, mean velocity profile

The following line indicates the values of surface roughness and friction velocity derived from the data of Figure 12. These parameters are required for simulation of the wind tunnel experiments with any CFD model.

Surface roughness = 0.00072 m Friction velocity = 0.035 m/s

Gas Concentration Data

Lateral profiles of gas concentration, all at 0.5 cm elevation, were made at several downwind distances for each of the Cases A-C. Downwind distances at which the lateral profiles were measured varied in order to ensure accurate determination of the distances associated with the concentrations representing the upper flammable limit (UFL), the lower flammable limit (LFL), and the one-half of the lower flammable limit (LFL/2). Also, in some cases the location of the measurement distances had to be varied slightly to avoid the concentration sensor touching a roughness element or the dike. Previous work (Havens and Spicer, 2003) had demonstrated excellent repeatability of the concentration measurements - data reproducibility is not presented here, as the confidence level in repeating the data is high.

Figures 13 - 15 are plots of the lateral profiles of concentration measured for Cases A, B, and C, respectively.

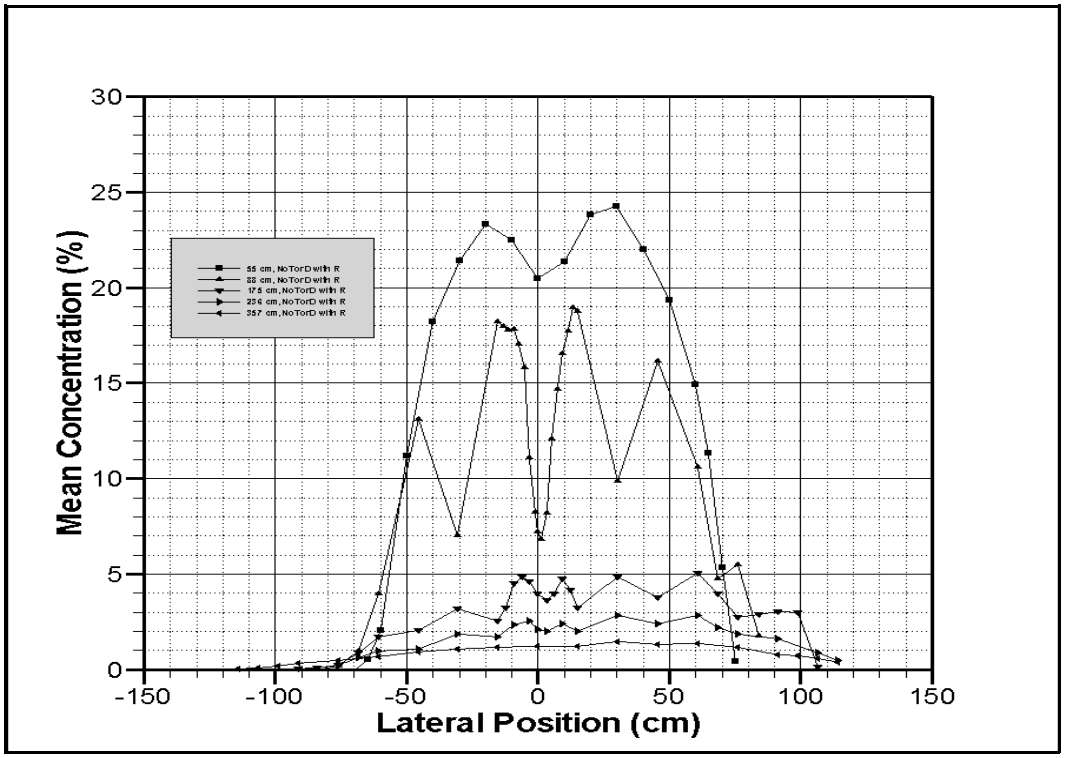

Figure 13. Lateral gas concentration profiles, 0.5 cm elevation - Case A

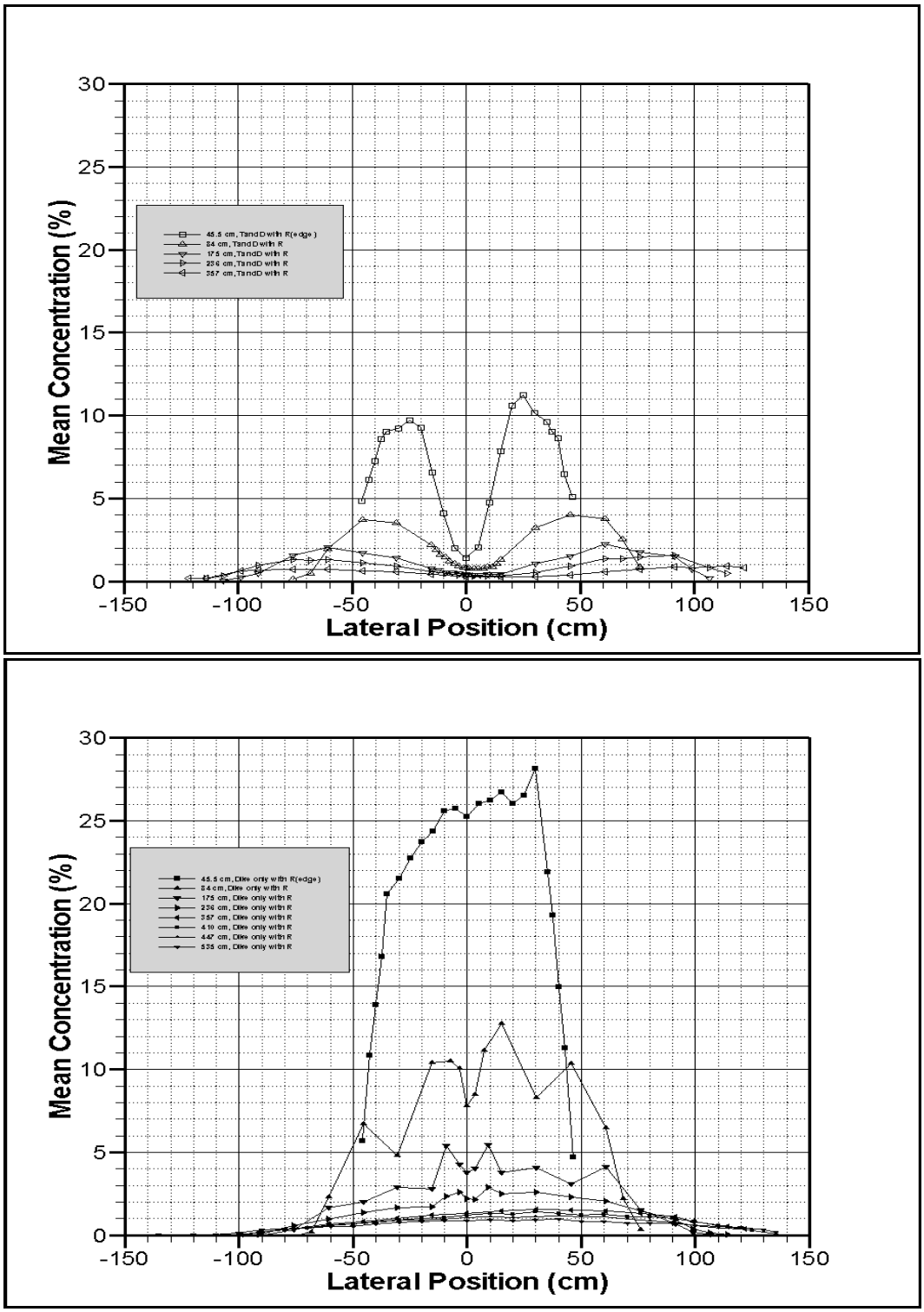

Figure 14. Lateral gas concentration profiles, 0.5 cm elevation - Case B (top)
Figure 15. Lateral gas concentration profiles, 0.5 cm elevation - Case C (bottom)

Below are summarized the maximum concentration values measured at the specified downwind locations for Cases A - C.

Case A: No tank or dike, with roughness

Downwind location (cm)	55	88	175	236	357
Maximum concentration (%)	24.2	18.9	5.1	2.8	1.4

Case B: Tank and Dike, with roughness

Downwind location (cm)	45.5	84	175	236	357
Maximum concentration (%)	11.23	4.0	2.3	1.6	0.90

Case C: Dike only, with roughness (45.5 cm distance is at downwind dike top edge)

Downwind location (cm)	45.5	84	175	236	357	410	447	535
Maximum concentration (%)	28.1	12.8	5.5	2.6	1.6	1.4	1.2	1.0

Observations and Discussion

Cases A, B, and C all show a slight shift of the plume to the right side of the tunnel. This result is highly repeatable and is believed to be the result, at least partly, of a very slight slope in the wind tunnel floor to the right hand side. This result has been observed throughout the fifteen-year working history of the tunnel. The wind tunnel floor was leveled to the nearest 1/100 inch during construction, but experience with dense gases indicates that slopes within this uncertainty could cause the observed shift. It is noted that slight position errors in centering the tank and elevations of the dike surfaces could also contribute to the shift observed to the right in the wind tunnel, as could possible slight pressure variations that persist due to minor differences in blockage in the area of return flow (it is impossible to place air/conditioning equipment and electrical conduits and raceways so that the blockage is completely uniform in the return space over, under, and around the tunnel cross section). Nevertheless, we do not consider this shift to be important, as it is rather slight, as long as the maximum concentration at a given downwind position is used for model evaluation.

Cases A, B, and C all show the expected more rapid dilution in the near field followed by less rapid dilution in the far field.

Case B clearly demonstrates the dilution in the near field that would be expected to result from the presence of obstacles (tank and dike) to the flow, showing the rapid dilution that occurs in the wake of the tank as a result of vertical mixing in the cloud over the length scale (height) of the tank. The tank also clearly causes bifurcation of the cloud, with near zero concentrations occurring at ground level on the centerline downwind of the tank and dike.

Case C demonstrates that an assumption that any obstruction (such as the dike in Case C) will result in greater dilution and corresponding shortening of the exclusion zone is by no means

certain, as it indicates a greater downwind travel distance with the dike than without (Case A), other factors being equal. Although this result was not expected, further analysis suggests that the dike restricts the gravity spreading of the cloud until the dike overflows, thus narrowing the cloud and reducing the overall top surface area of the cloud. As it is known that gravity spreading can decrease downwind maximum distances traveled (while resulting in a wider cloud with greater cloud coverage area), Case C indicates that restriction of gravity spreading explains the unexpected greater travel distance observed with the dike. Comparison of Figures 13 and 15 indicates the restriction on gravity spreading and resultant narrowing of the cloud in the area of the dike. It is emphasized that CFD models should provide for this effect, but that bulk parameter models (similar to DEGADIS) would not be expected to cope.

This work clearly demonstrates the importance of the site roughness. The field scaled roughness value corresponding to the wind tunnel roughness would be about 11 cm, which is significantly higher than the 3 cm value typically recommended for a grassy site surrounding an LNG terminal. Comparison with earlier measurements on the CHRC tunnel smooth floor suggest that this large surface roughness alone is decreasing the downwind travel distance by roughly the same amount as the presence of the tank and dike (on the smooth floor) alone. Consequently, the large roughness effect, particularly for Case C, should not be considered typical. It is noted that the spikiness in the intermediate downwind distance lateral gas concentration profiles shown for Cases A and C is very repeatable and correlates with the position of the gas sampling probe being in or out of the wake of a roughness element. As expected, the greater dilution that occurs at these distances in Case B results in smoothing of this effect, and the spikes are not observed, even though the gas concentrations were made in the same locations as for Cases A and C.

CFD models, or for that matter, DEGADIS, can and should be used with the roughness appropriate to the site under consideration. The large roughness here is designed to result in a wind tunnel boundary layer that is scalable to field conditions. We believe that the smooth floor wind tunnel dense-gas dispersion data previously reported (Havens and Spicer, 2003), although useful for limited mathematical model validation, should not be scaled to field conditions, for the reasons stated earlier in this report. However we are confident that the rough floor wind tunnel data reported herein does not suffer that weakness. The CHRC can provide interested parties extensive background on the development of the surface roughness used in this work, as its development and testing was undertaken in a joint program by the University of Arkansas and the Environmental Protection Agency's Environmental Wind Tunnel in North Carolina for the Petroleum Energy Research Foundation (Havens et.al., 2001: Briggs et.al., 2001).

5.0 CONCLUSIONS AND RECOMMENDATIONS

This subcontract specified three principal tasks.

The objective of Task A was to eliminate stability problems that had been observed in FEM3A simulations of low-wind-speed, stably-stratified conditions. This was a high priority requirement since the application of the code for compliance with the regulation can require simulations to be made for such conditions, which are sometimes worst case. Task A was completed, and a new version of FEM3A, free of the aforementioned stability problems, is being provided to GTI.

The objective of Task B was to repeat and extend former experiments using uniform roughness elements covering the wind tunnel floor to create turbulence properties similar to field scale wind conditions and to develop and verify a k-epsilon turbulence closure model that allows for more realistic description of dispersion problems with obstacle and terrain effects. Task B was completed; this report contains the data produced, and a new version of FEM3A with the improved k-epsilon closure is being provided to GTI.

The original objective of Task C was to adapt the FEM3A model for more general application; however, near the mid-point of the contract period, DOE redirected this effort in order to provide CHRC's assistance to DOE-NETL in their consideration of the FLUENT CFD model as an alternative to FEM3A. Consequently, this task was obviated, and Task D was added.

The objective of Task D was to provide assistance and wind tunnel data to DOE for FLUENT development. Task D was completed and data requested by DOE-NETL was delivered.

This report contains a summary of wind tunnel data for rough-wind-tunnel-floor simulation of three gas dense dispersion scenarios applicable to determination of LNG vapor cloud dispersion exclusion zone determinations:

Case A. Low momentum area source CO_2 release without obstacles
Case B. Low momentum area source CO_2 release with dike and tank
Case C. Low momentum area source CO_2 release with dike only

Cases A, B, and C all show the expected more rapid dilution in the near field followed by less rapid dilution in the far field.

Case B clearly demonstrates the dilution in the near field that is expected to result from the presence of obstacles (tank and dike) to the flow. Case B also indicates bifurcation of the cloud by the flow around the tank, with near zero concentrations occurring at ground level on the centerline downwind of the tank and dike.

Case C demonstrates that an assumption that any obstruction (such as the dike in Case C) will result in greater dilution and corresponding shortening of the exclusion zone is by no means

certain. Case C indicates a greater downwind travel distance with the dike than without (Case A), other factors being equal. As it is known that gravity spreading can decrease downwind maximum distances traveled, while resulting in greater cloud coverage area, Case C indicates this explanation of the unexpected greater travel distance observed with the dike than without the dike.

The importance of site roughness is clearly demonstrated. The field scaled roughness value corresponding to the wind tunnel roughness reported here would be about 11 cm, which is significantly higher than the 3 cm value typically recommended for a grassy site surrounding an LNG terminal. Consequently, the large roughness effect shown here should not be considered typical. The FEM3A (or other CFD model), or for that matter, DEGADIS, can and should be used with the roughness appropriate to the site under consideration.

The large roughness here is designed to result in a wind tunnel boundary layer that is scalable to field conditions. We are not confident that the smooth floor wind tunnel dense-gas dispersion data previously reported, although useful for limited mathematical model validation, can be scaled to field conditions. However we are confident that the rough floor wind tunnel data reported herein does not suffer that weakness, and the use of data reported in Cases A, B, and C are recommended for CFD model evaluation, either by direct simulation at wind tunnel scale, or by simulation at field (150/1) scale for comparison with the scaled wind tunnel data.

We have utilized the FEM3A model throughout in order to consider the utility of this data for verification of CFD models, as well as to continue our own in-house improvement and maintenance of FEM3A. Based on our observations, we recommend the following considerations regarding the use of this data for verifying CFD models, and for the use of approved methods for determining LNG vapor cloud exclusion zones:

- The wind tunnel data appears to be in best agreement in the near field, with increasing differences appearing in the (unobstructed) far field. Considering that the k-epsilon method used here would appear to be better suited to the near field calculation than the far field because its sensitivity to ad hoc provisions for density stratification, we believe that the turbulence closure approach used in the far field should be further evaluated in order to better characterize the effects upon density stratification on determinations of the turbulent kinetic energy (k) and the turbulence kinetic energy dissipation rate (epsilon).

- As a consequence of this finding, we recommend that FEM3A be used to determine the gas/air concentration and rate that overflows the downwind dike edge, and that the result be used as input to DEGADIS for determining the distance from the downwind edge of the dike to the ½ lfl concentration level prescribed by 49 CFR 193. We have demonstrated this method, providing further justification for this recommendation, in a recent publication in the AICHE organ Plant Safety Progress (Havens and Spicer, 2005).

REFERENCES

Arthur D. Little, Inc., “Evaluation of LNG Vapor Control Methods”, Report to the American Gas Association, October, 1974.

Havens, J. A., T. O. Spicer, and P.J. Schreurs, “Evaluation of 3-D Hydrodynamic Computer Models for Prediction of LNG Vapor Dispersion in the Atmosphere,” Final Report to GRI on Contract No. 5083-252-0788, August, 1987.

Havens, Jerry and Tom Spicer, “LNG Vapor Dispersion Prediction with the DEGADIS Dense Gas Dispersion Model,” Topical Report to GRI on Contract No. 5086-252-1287, September 1990.

Havens, Jerry, Tom Spicer, and Heather Walker, “ Regulatory Application of Wind Tunnel Models and Complex Mathematical Models for Simulating Atmospheric Dispersion of LNG Vapor,” Gas Research Institute Report No. 92-0257, August 1994.

Havens, Jerry, Tom Spicer, and Heather Walker, “Evaluation of Mitigation Methods for Accidental LNG Releases: Volume 1/5–Wind Tunnel Experiments and Mathematical Model Simulations to Study Dispersion of a Vapor Cloud Formed following LNG Spillage into a Diked Area Surrounding a Storage Tank,” Topical Report for Gas Research Institute, November 1996.

Havens, Jerry, Tom Spicer, and Heather Walker, “Evaluation of Mitigation Methods for Accidental LNG Releases: Volume 2/5– Wind Tunnel Experiments and Mathematical Model Simulations to Study Heat Transfer from a Flat Surface to a Cold Nitrogen Cloud in a Simulated Atmospheric Boundary Layer,” Topical Report for Gas Research Institute, November 1996.

Havens, Jerry, Tom Spicer, and Heather Walker, “Evaluation of Mitigation Methods for Accidental LNG Releases: Volume 3/5– Wind Tunnel Experiments for Mitsubishi Heavy Industries, Ltd.,” Topical Report for Gas Research Institute, November 1996.

Havens, Jerry, Tom Spicer, and Heather Walker, “Evaluation of Mitigation Methods for Accidental LNG Releases: Volume 4/5–Wind Tunnel Experiments for Osaka Gas Company,” Topical Report for Gas Research Institute, November 1996.

Spicer, Tom, Jerry Havens, and Heather Walker, “Evaluation of Mitigation Methods for Accidental LNG Releases: Volume 5/5–Using FEM3A for LNG Accident Consequence Analysis,” Topical Report for Gas Research Institute, December 1996.

Havens, J. A., H. L. Walker, and T. O. Spicer, “Wind Tunnel Study of Air Entrainment Into Two-Dimensional Dense Gas Plumes at the Chemical Hazards Research Center,” Atmospheric Environment, 35, 2001.

Briggs, G. A., R. E. Britter, S. R. Hanna, J. A. Havens, A. G. Robins, and W. H. Synder, "Dense Gas Vertical Diffusion Over Rough Surfaces: Results of Wind-Tunnel Studies," Atmospheric Environment, 35, 2001.

Havens, Jerry, and Tom Spicer, "Evaluation of Mitigation Methods for Accidental LNG Releases - The FEM3A Model: Continuing Wind Tunnel Verification," Final Topical Report to Gas Technology Institute on Contract 5091-252-2272, March 2003.

Havens, J. And T. Spicer, "LNG Vapor Dispersion in Impoundments", Plant Safety Progress, Vol. 24, No.3, September 2005.

Appendix I

Wind Tunnel Illustrations and Model Details

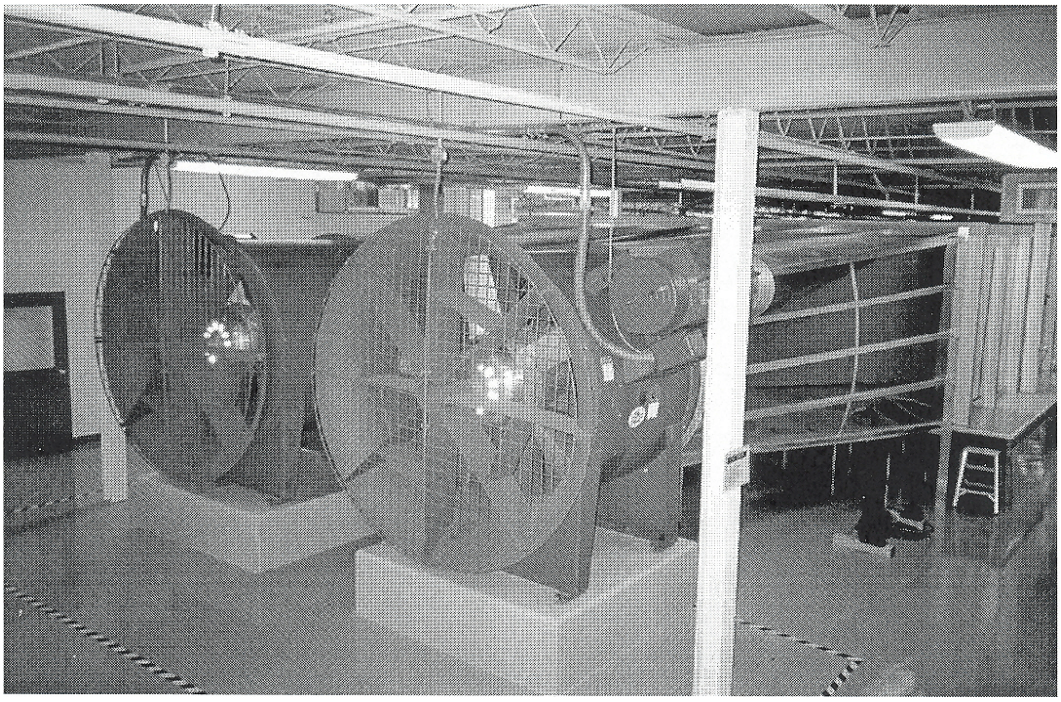

Figure I-1 Illustration of dual fans

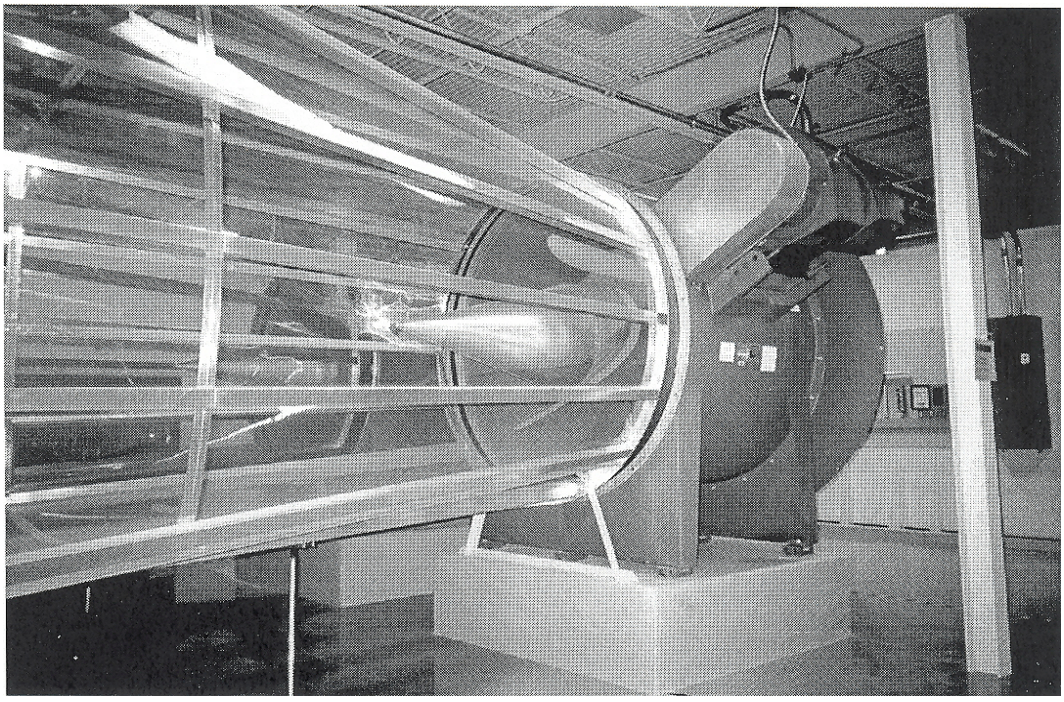

Figure I-2 Illustration of fan-to-tunnel transition

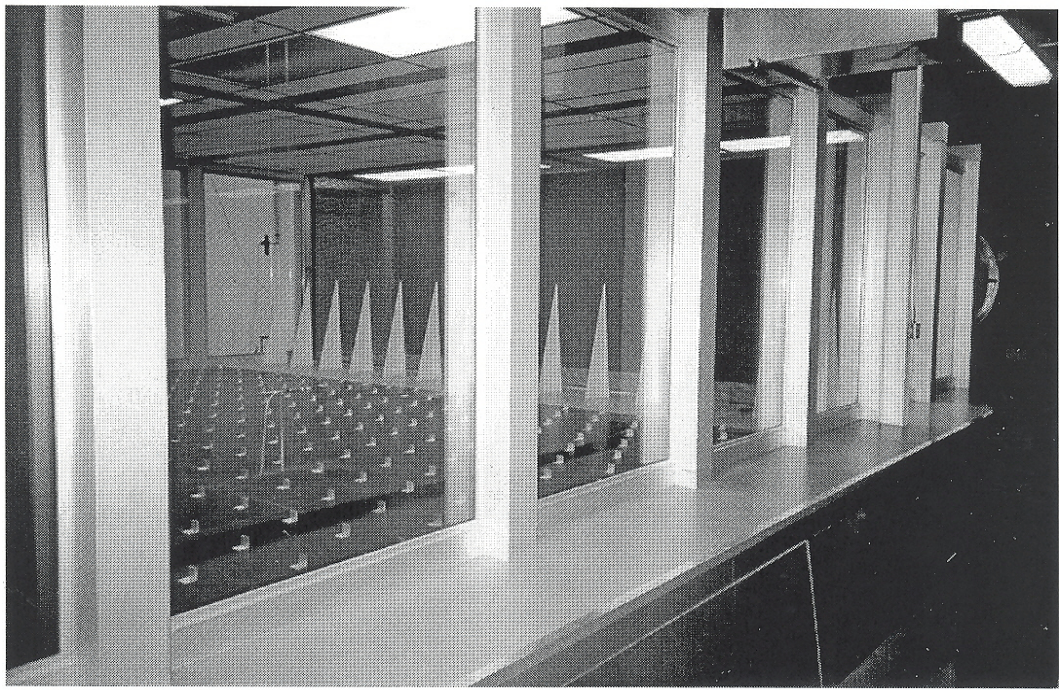

Figure I-3. Illustration of boundary layer generation section

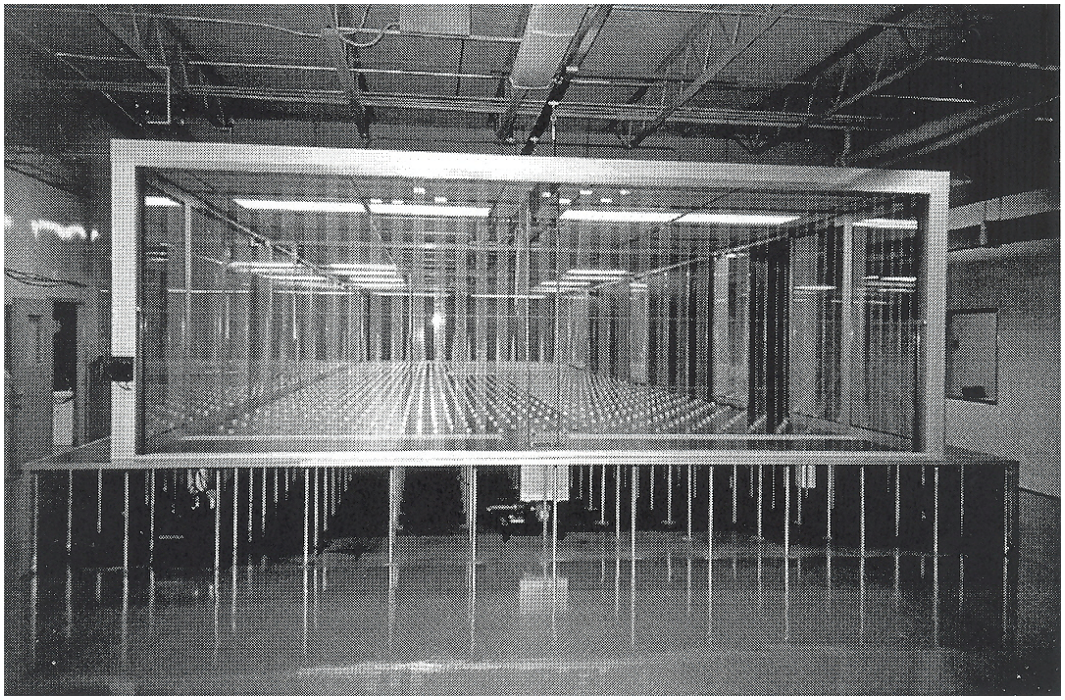

Figure I-4. Illustration of back pressure device at end of tunnel

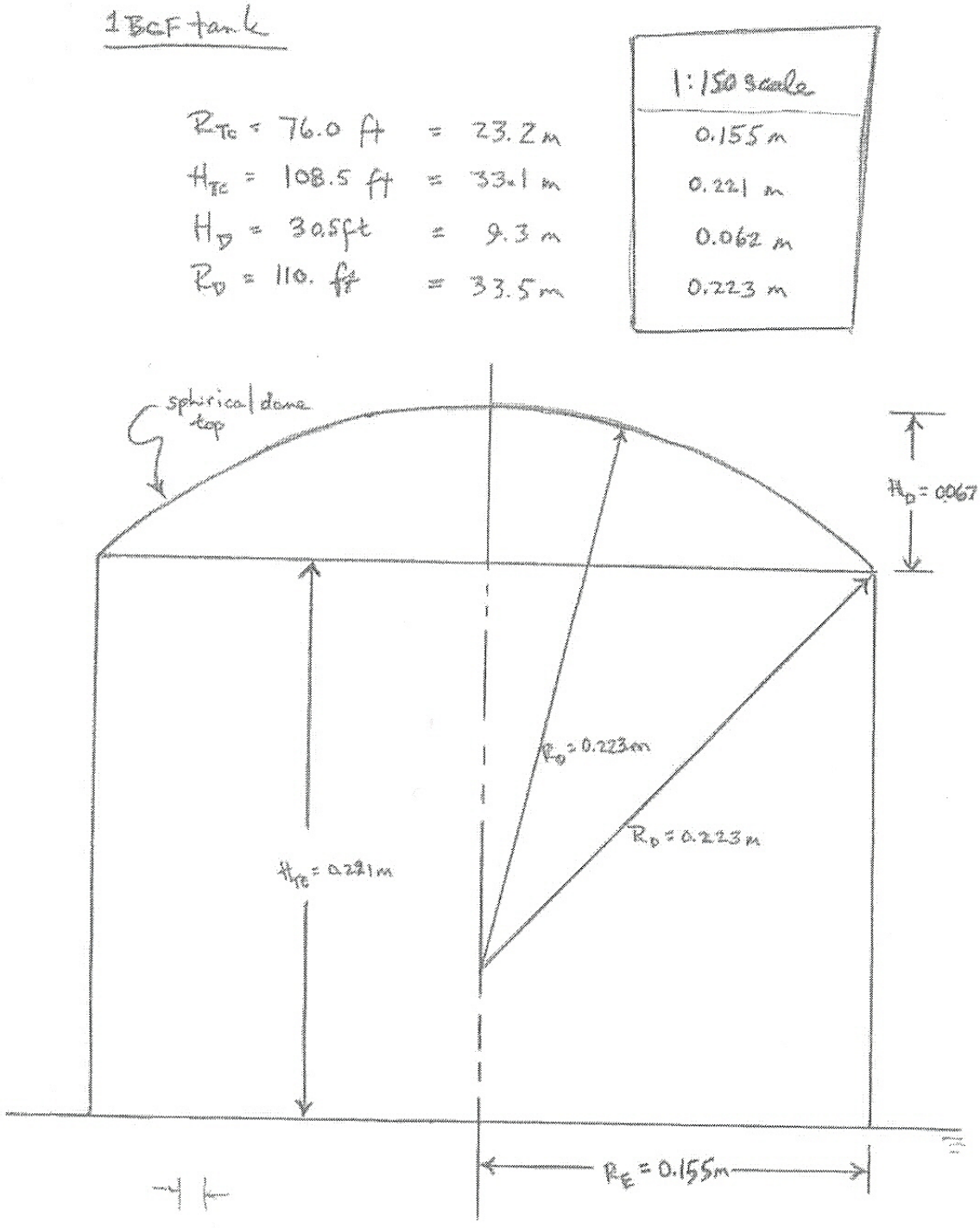

Figure I-5. Details of model LNG tank

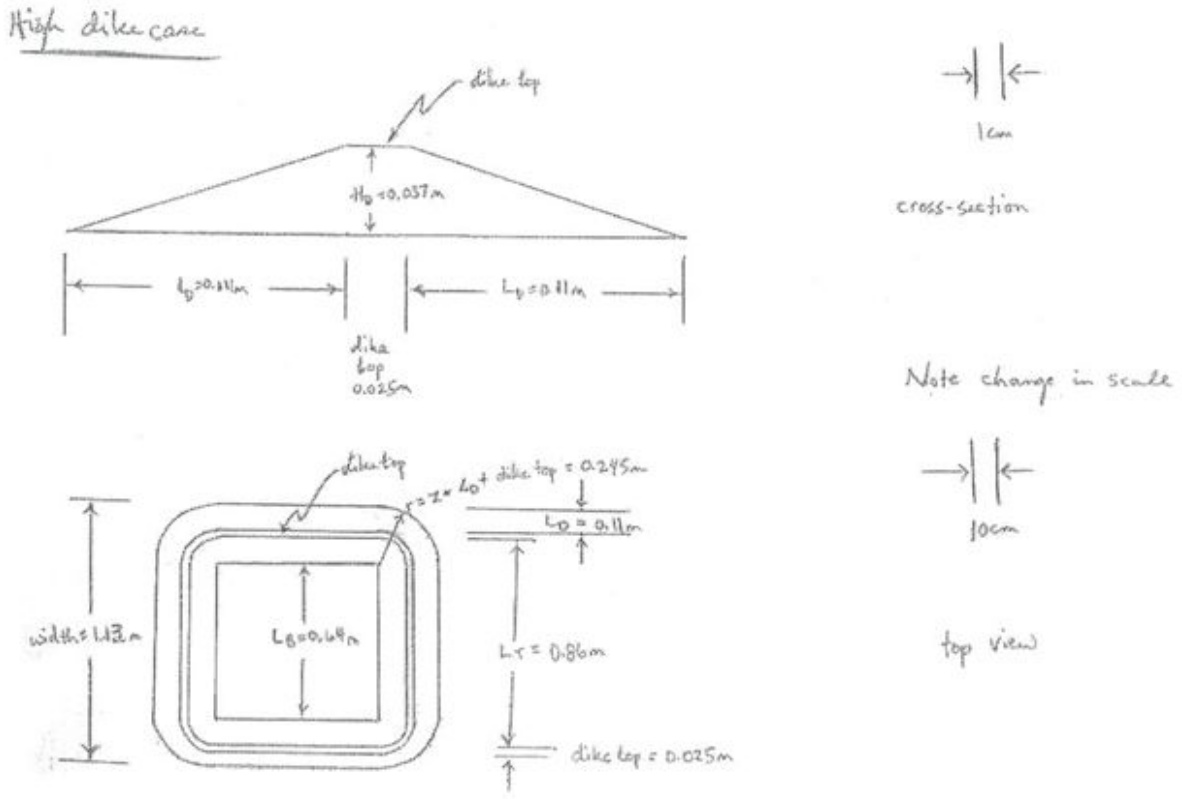

Figure I-6. Details of model LNG dike

Appendix II

Experimental Data

Table II.1. Approach flow mean velocity data

Vertical Profile of Approach Flow Mean Velocity - Rough Wind Tunnel Floor

Height (cm)	Velocity (m/s)
0.5	0.2078
0.95	0.2666
1.5	0.3079
2.3	0.3204
3.3	0.3484
4.6	0.3668
6.3	0.3906
8.5	0.4194
11.5	0.4516
15	0.4881
20	0.4953

Table II.2. Gas concentration data for low momentum area source CO_2 release - rough surface boundary layer - Case A

Data Set A1 - Lateral Concentration Profile @ 55 cm downwind of source center

X (cm)	Y (cm)	Z (cm)	Mean Conc. (%)
55	-75	0.5	-0.02
55	-70	0.5	-0.02
55	-65	0.5	0.53
55	-60	0.5	2.04
55	-50	0.5	11.19
55	-40	0.5	18.2
55	-30	0.5	21.42
55	-20	0.5	23.34
55	-10	0.5	22.5
55	0	0.5	20.48
55	10	0.5	21.35
55	20	0.5	23.81
55	30	0.5	24.24
55	40	0.5	22
55	50	0.5	19.36
55	60	0.5	14.91
55	65	0.5	11.32
55	70	0.5	5.34
55	75	0.5	0.45

Table II.2. Gas concentration data for low momentum area source CO_2 release - rough surface boundary layer - Case A (continued)

Data Set A2 - Lateral Concentration Profile @ 88 cm downwind of source center

X (cm)	Y (cm)	Z (cm)	Mean Conc. (%)
88	-84.06	0.5	-0.01
88	-76.2	0.5	0.18
88	-68.58	0.5	0.95
88	-60.96	0.5	3.96
88	-45.72	0.5	13.1
88	-30.48	0.5	7.02
88	-15.24	0.5	18.2
88	-13.24	0.5	17.98
88	-11.24	0.5	17.77
88	-9.24	0.5	17.81
88	-7.24	0.5	17.05
88	-5.24	0.5	15.79
88	-3.24	0.5	11.08
88	-1.24	0.5	8.26
88	0	0.5	7.21
88	1.24	0.5	6.82
88	3.24	0.5	8.2
88	5.24	0.5	12.07
88	7.24	0.5	14.69
88	9.24	0.5	16.53
88	11.24	0.5	17.71
88	13.24	0.5	18.93
88	15.24	0.5	18.77
88	30.48	0.5	9.86
88	45.72	0.5	16.14
88	60.96	0.5	10.6
88	68.58	0.5	4.75
88	76.2	0.5	5.5
88	84.06	0.5	1.74

Table II.2. Gas concentration data for low momentum area source CO_2 release - rough surface boundary layer - Case A (continued)

Data Set A3 - Lateral Concentration Profile @ 175 cm downwind of source center

X (cm)	Y (cm)	Z (cm)	Mean Conc. (%)
175	-91.43	0.5	0.03
175	-84.06	0.5	0.07
175	-76.2	0.5	0.25
175	-68.58	0.5	0.87
175	-60.96	0.5	1.69
175	-45.72	0.5	2.04
175	-30.48	0.5	3.17
175	-15.24	0.5	2.56
175	-12.24	0.5	3.22
175	-9.24	0.5	4.51
175	-6.24	0.5	4.87
175	-3.24	0.5	4.63
175	0	0.5	3.98
175	3.24	0.5	3.62
175	6.24	0.5	3.99
175	9.24	0.5	4.73
175	12.24	0.5	4.16
175	15.24	0.5	3.23
175	30.48	0.5	4.84
175	45.72	0.5	3.75
175	60.96	0.5	5.05
175	68.58	0.5	3.99
175	76.2	0.5	2.72
175	84.07	0.5	2.87
175	91.43	0.5	3.01
175	99.06	0.5	2.99
175	106.69	0.5	0.14

Table II.2. Gas concentration data for low momentum area source CO_2 release - rough surface boundary layer - Case A (continued)

Data Set A4 - Lateral Concentration Profile @ 236 cm downwind of source center

X (cm)	Y (cm)	Z (cm)	Mean Conc. (%)
236	-106.68	0.5	-0.04
236	-91.43	0.5	-0.02
236	-76.2	0.5	0.24
236	-68.58	0.5	0.62
236	-60.96	0.5	0.98
236	-45.72	0.5	1.09
236	-30.48	0.5	1.83
236	-15.24	0.5	1.7
236	-9.24	0.5	2.35
236	-3.24	0.5	2.55
236	0	0.5	2.12
236	3.24	0.5	2.01
236	9.24	0.5	2.37
236	15.24	0.5	1.99
236	30.48	0.5	2.83
236	45.72	0.5	2.4
236	60.96	0.5	2.82
236	68.58	0.5	2.21
236	76.2	0.5	1.83
236	91.43	0.5	1.6
236	106.69	0.5	0.85
236	114.3	0.5	0.49

Table II.2. Gas concentration data for low momentum area source CO_2 release - rough surface boundary layer - Case A (continued)

Data Set A5 - Lateral Concentration Profile @ 357 cm downwind of source center

X (cm)	Y (cm)	Z (cm)	Mean Conc. (%)
357	-114.3	0.5	0.02
357	-106.68	0.5	0.08
357	-99.06	0.5	0.17
357	-91.44	0.5	0.32
357	-76.2	0.5	0.46
357	-60.96	0.5	0.69
357	-45.72	0.5	0.91
357	-30.48	0.5	1.06
357	-15.24	0.5	1.15
357	0	0.5	1.23
357	15.24	0.5	1.23
357	30.48	0.5	1.44
357	45.72	0.5	1.3
357	60.96	0.5	1.35
357	76.2	0.5	1.17
357	91.44	0.5	0.79
357	99.06	0.5	0.71
357	106.68	0.5	0.59
357	114.3	0.5	0.38

Table II.3. Gas concentration data for low momentum area source CO_2 release with model tank and dike - rough surface boundary layer - Case B

Data Set B1 - Lateral Concentration Profile @ 45.5 cm downwind of source center

X (cm)	Y (cm)	Z (cm)	Mean Conc. (%)
45.5	-46	3.18	4.85
45.5	-43	3.18	6.15
45.5	-40	3.18	7.27
45.5	-37.5	3.18	8.61
45.5	-35	3.18	9.02
45.5	-30	3.18	9.22
45.5	-25	3.18	9.74
45.5	-20	3.18	9.27
45.5	-15	3.18	6.56
45.5	-10	3.18	4.13
45.5	-5	3.18	2
45.5	0	3.18	1.42
45.5	5	3.18	2.06
45.5	10	3.18	4.76
45.5	15	3.18	7.85
45.5	20	3.18	10.62
45.5	25	3.18	11.23
45.5	30	3.18	10.18
45.5	35	3.18	9.61
45.5	37.5	3.18	9.04
45.5	40	3.18	8.64
45.5	43	3.18	6.49
45.5	46.5	3.18	5.1

Table II.3. Gas concentration data for low momentum area source CO_2 release with model tank and dike - rough surface boundary layer - Case B (continued)

Data Set B2 - Lateral Concentration Profile @ 84 cm downwind of source center

X (cm)	Y (cm)	Z (cm)	Mean Conc. (%)
84	-76.2	0.5	0.14
84	-68.58	0.5	0.5
84	-60.96	0.5	1.96
84	-45.72	0.5	3.72
84	-30.48	0.5	3.53
84	-15.24	0.5	2.19
84	-13.24	0.5	1.88
84	-11.24	0.5	1.63
84	-9.24	0.5	1.44
84	-7.24	0.5	1.22
84	-5.24	0.5	1.07
84	-3.24	0.5	0.94
84	-1.24	0.5	0.83
84	0	0.5	0.8
84	1.24	0.5	0.78
84	3.24	0.5	0.77
84	5.24	0.5	0.78
84	7.24	0.5	0.79
84	9.24	0.5	0.88
84	11.24	0.5	0.88
84	13.24	0.5	1.07
84	15.24	0.5	1.29
84	30.48	0.5	3.24
84	45.72	0.5	4.03
84	60.96	0.5	3.75
84	68.58	0.5	2.54
84	76.2	0.5	0.88

Table II.3. Gas concentration data for low momentum area source CO_2 release with model tank and dike - rough surface boundary layer - Case B (continued)

Data Set B3 - Lateral Concentration Profile @ 175 cm downwind of source center

X (cm)	Y (cm)	Z (cm)	Mean Conc. (%)
175	-106.68	0.5	0.02
175	-99.06	0.5	0.22
175	-91.44	0.5	0.46
175	-76.2	0.5	1.54
175	-60.96	0.5	2.07
175	-45.72	0.5	1.72
175	-30.48	0.5	1.4
175	-15.24	0.5	0.76
175	-12.24	0.5	0.65
175	-9.24	0.5	0.54
175	-6.24	0.5	0.51
175	-3.24	0.5	0.46
175	0	0.5	0.41
175	3.24	0.5	0.4
175	6.24	0.5	0.36
175	9.24	0.5	0.44
175	12.24	0.5	0.45
175	15.24	0.5	0.44
175	30.48	0.5	1.09
175	45.72	0.5	1.52
175	60.96	0.5	2.26
175	76.2	0.5	1.74
175	91.44	0.5	1.49
175	99.06	0.5	0.72
175	106.68	0.5	0.19

Table II.3. Gas concentration data for low momentum area source CO_2 release with model tank and dike - rough surface boundary layer - Case B (continued)

Data Set B4 - Lateral Concentration Profile @ 236 cm downwind of source center

X (cm)	Y (cm)	Z (cm)	Mean Conc. (%)
236	-114.3	0.5	0.18
236	-106.68	0.5	0.32
236	-91.44	0.5	0.99
236	-76.2	0.5	1.3
236	-68.58	0.5	1.28
236	-60.96	0.5	1.3
236	-45.72	0.5	1.1
236	-30.48	0.5	0.94
236	-15.24	0.5	0.58
236	-9.24	0.5	0.48
236	-3.24	0.5	0.38
236	0	0.5	0.34
236	3.24	0.5	0.32
236	9.24	0.5	0.32
236	15.24	0.5	0.32
236	30.48	0.5	0.53
236	45.72	0.5	0.94
236	60.96	0.5	1.34
236	68.58	0.5	1.37
236	76.2	0.5	1.46
236	91.44	0.5	1.55
236	106.68	0.5	0.84
236	114.3	0.5	0.46

Table II.3. Gas concentration data for low momentum area source CO_2 release with model tank and dike - rough surface boundary layer - Case B (continued)

Data Set B5 - Lateral Concentration Profile @ 357 cm downwind of source center

X (cm)	Y (cm)	Z (cm)	Mean Conc. (%)
357	-121.92	0.5	0.16
357	-114.3	0.5	0.2
357	-99.06	0.5	0.61
357	-91.44	0.5	0.68
357	-76.2	0.5	0.74
357	-60.96	0.5	0.7
357	-45.72	0.5	0.64
357	-30.48	0.5	0.58
357	-15.24	0.5	0.42
357	0	0.5	0.3
357	15.24	0.5	0.26
357	30.48	0.5	0.3
357	45.72	0.5	0.38
357	60.96	0.5	0.56
357	76.2	0.5	0.73
357	91.44	0.5	0.86
357	99.06	0.5	0.84
357	114.3	0.5	0.9
357	121.92	0.5	0.84

Table II.4. Gas concentration data for low momentum area source CO_2 release with model dike only - rough surface boundary layer - Case C

Data Set C1 - Lateral Concentration Profile @ 45.5 cm downwind of source center

X (cm)	Y (cm)	Z (cm)	Mean Conc. (%)
45.5	-46	0.5	5.7
45.5	-43	0.5	10.83
45.5	-40	0.5	13.87
45.5	-37.5	0.5	16.78
45.5	-35	0.5	20.56
45.5	-30	0.5	21.5
45.5	-25	0.5	22.75
45.5	-20	0.5	23.73
45.5	-15	0.5	24.34
45.5	-10	0.5	25.58
45.5	-5	0.5	25.75
45.5	0	0.5	25.23
45.5	5	0.5	26.05
45.5	10	0.5	26.24
45.5	15	0.5	26.71
45.5	20	0.5	26.03
45.5	25	0.5	26.52
45.5	30	0.5	28.13
45.5	35	0.5	21.92
45.5	37.5	0.5	19.32
45.5	40	0.5	14.97
45.5	43	0.5	11.27
45.5	46.5	0.5	4.69

Table II.4. Gas concentration data for low momentum area source CO_2 release with model dike only - rough surface boundary layer - Case C (continued)

Data Set C2 - Lateral Concentration Profile @ 84 cm downwind of source center

X (cm)	Y (cm)	Z (cm)	Mean Conc. (%)
84	-76.2	0.5	-0.04
84	-68.58	0.5	0.2
84	-60.96	0.5	2.32
84	-45.72	0.5	6.71
84	-30.48	0.5	4.82
84	-15.24	0.5	10.42
84	-7.24	0.5	10.52
84	-3.24	0.5	10.06
84	0	0.5	7.8
84	3.24	0.5	8.47
84	7.24	0.5	11.16
84	15.24	0.5	12.78
84	30.48	0.5	8.28
84	45.72	0.5	10.34
84	60.96	0.5	6.48
84	68.58	0.5	2.2
84	76.2	0.5	0.35

Table II.4. Gas concentration data for low momentum area source CO_2 release with model dike only - rough surface boundary layer - Case C (continued)

Data Set C3 - Lateral Concentration Profile @ 175 cm downwind of source center

X (cm)	Y (cm)	Z (cm)	Mean Conc. (%)
175	-106.68	0.5	-0.04
175	-99.06	0.5	-0.04
175	-91.44	0.5	-0.04
175	-76.2	0.5	0.34
175	-60.96	0.5	1.67
175	-45.72	0.5	1.98
175	-30.48	0.5	2.88
175	-15.24	0.5	2.78
175	-9.24	0.5	5.39
175	-3.24	0.5	4.27
175	0	0.5	3.79
175	3.24	0.5	4.01
175	9.24	0.5	5.46
175	15.24	0.5	3.77
175	30.48	0.5	4.05
175	45.72	0.5	3.09
175	60.96	0.5	4.12
175	76.2	0.5	1.52
175	91.44	0.5	0.65
175	99.06	0.5	0.16
175	106.68	0.5	0.04

Table II.4. Gas concentration data for low momentum area source CO_2 release with model dike only - rough surface boundary layer - Case C (continued)

Data Set C4 - Lateral Concentration Profile @ 236 cm downwind of source center

X (cm)	Y (cm)	Z (cm)	Mean Conc. (%)
236	-114.3	0.5	-0.06
236	-106.68	0.5	-0.05
236	-99.06	0.5	-0.04
236	-91.44	0.5	0.05
236	-76.2	0.5	0.56
236	-60.96	0.5	0.98
236	-45.72	0.5	1.35
236	-30.48	0.5	1.68
236	-15.24	0.5	1.73
236	-9.24	0.5	2.34
236	-3.24	0.5	2.59
236	0	0.5	2.2
236	3.24	0.5	2.14
236	9.24	0.5	2.9
236	15.24	0.5	2.5
236	30.48	0.5	2.58
236	45.72	0.5	2.32
236	60.96	0.5	2.04
236	76.2	0.5	1.48
236	91.44	0.5	0.91
236	99.06	0.5	0.37
236	106.68	0.5	0.11
236	114.3	0.5	0.06

Table II.4. Gas concentration data for low momentum area source CO_2 release with model dike only - rough surface boundary layer - Case C (continued)

Data Set C5 - Lateral Concentration Profile @ 357 cm downwind of source center

X (cm)	Y (cm)	Z (cm)	Mean Conc. (%)
357	-121.93	0.5	-0.01
357	-114.3	0.5	-0.02
357	-99.06	0.5	0.05
357	-91.44	0.5	0.16
357	-76.2	0.5	0.36
357	-60.96	0.5	0.68
357	-45.72	0.5	0.83
357	-30.48	0.5	1.02
357	-15.24	0.5	1.2
357	0	0.5	1.3
357	15.24	0.5	1.45
357	30.48	0.5	1.57
357	45.72	0.5	1.52
357	60.96	0.5	1.44
357	76.2	0.5	1.3
357	91.44	0.5	1.12
357	99.06	0.5	0.8
357	114.3	0.5	0.51
357	121.93	0.5	0.4

Table II.4. Gas concentration data for low momentum area source CO_2 release with model dike only - rough surface boundary layer - Case C (continued)

Data Set C6 - Lateral Concentration Profile @ 410 cm downwind of source center

X (cm)	Y (cm)	Z (cm)	Mean Conc. (%)
410	-125	0.5	-0.02
410	-110	0.5	-0.02
410	-100	0.5	0
410	-90	0.5	0.2
410	-80	0.5	0.33
410	-70	0.5	0.42
410	-60	0.5	0.6
410	-50	0.5	0.65
410	-40	0.5	0.79
410	-30	0.5	0.92
410	-20	0.5	1.02
410	-10	0.5	1.07
410	0	0.5	1.22
410	10	0.5	1.29
410	20	0.5	1.26
410	30	0.5	1.4
410	40	0.5	1.29
410	50	0.5	1.22
410	60	0.5	1.28
410	70	0.5	1.12
410	80	0.5	1.1
410	90	0.5	1.04
410	100	0.5	0.84
410	110	0.5	0.59
410	125	0.5	0.28

Table II.4. Gas concentration data for low momentum area source CO_2 release with model dike only - rough surface boundary layer - Case C (continued)

Data Set C7 - Lateral Concentration Profile @ 447 cm downwind of source center

X (cm)	Y (cm)	Z (cm)	Mean Conc. (%)
447	-135	0.5	-0.02
447	-130	0.5	-0.02
447	-120	0.5	0
447	-110	0.5	-0.04
447	-100	0.5	0.06
447	-90	0.5	0.18
447	-80	0.5	0.36
447	-70	0.5	0.42
447	-60	0.5	0.64
447	-50	0.5	0.66
447	-40	0.5	0.8
447	-30	0.5	0.93
447	-20	0.5	0.94
447	-10	0.5	0.96
447	0	0.5	1.08
447	10	0.5	1.1
447	20	0.5	1.07
447	30	0.5	1.12
447	40	0.5	1.16
447	50	0.5	1.12
447	60	0.5	1.12
447	70	0.5	0.98
447	80	0.5	0.88
447	90	0.5	0.76
447	100	0.5	0.59
447	110	0.5	0.45
447	120	0.5	0.4
447	130	0.5	0.16
447	135	0.5	0.09

Table II.4. Gas concentration data for low momentum area source CO_2 release with model dike only - rough surface boundary layer - Case C (continued)

Data Set C8 - Lateral Concentration Profile @ 535 cm downwind of source center

X (cm)	Y (cm)	Z (cm)	Mean Conc. (%)
535	-135	0.5	0.03
535	-130	0.5	-0.01
535	-120	0.5	0.03
535	-110	0.5	0.05
535	-100	0.5	0.12
535	-90	0.5	0.31
535	-80	0.5	0.4
535	-70	0.5	0.44
535	-60	0.5	0.55
535	-50	0.5	0.54
535	-40	0.5	0.68
535	-30	0.5	0.77
535	-20	0.5	0.82
535	-10	0.5	0.86
535	0	0.5	0.86
535	10	0.5	0.93
535	20	0.5	0.88
535	30	0.5	0.9
535	40	0.5	0.96
535	50	0.5	0.82
535	60	0.5	0.82
535	70	0.5	0.71
535	80	0.5	0.72
535	90	0.5	0.7
535	100	0.5	0.59
535	110	0.5	0.54
535	120	0.5	0.47
535	130	0.5	0.34
535	135	0.5	0.17